AD-A117 901 ULTRASONICS INTERNATIONAL INC TREVOSE PA F/G 11/6
ULTRASONIC MEASUREMENT OF CASE DEPTH IN CASE HARDENED STEELS. E--ETC(U)
JUL 82 M S GOOD N00014-82-C-0144
UNCLASSIFIED NL

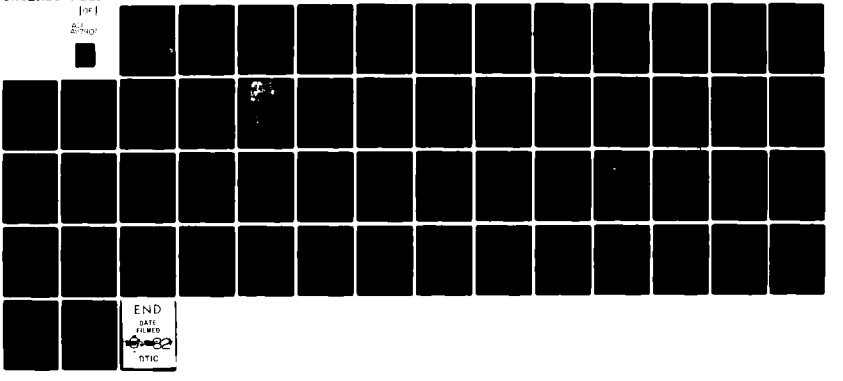

END
DATE FILMED
-82
DTIC

(12)

Report N00014-82-C-0144

ULTRASONIC MEASUREMENT OF CASE DEPTH IN CASE HARDENED STEELS

Evaluation of Feasibility for the Ultrasonic Measurement of Case Depth in Case Hardened Steels

Morris S. Good
Ultrasonics International, Inc.
Three Neshaminy Interplex, Suite 215
Trevose, Pennsylvania 19047

July 1982

Final Report for Period January 1982 - June 1982

Prepared for

NAVAL RESEARCH LABORATORY
Code 2627
Washington, D. C. 20375

OFFICE OF NAVAL RESEARCH
Eastern/Central Regional Office
666 Summer Street
Boston, Massachusetts 02210

MIL-STD-847A
31 January 1973

Unclassified
SECURITY CLASSIFICATION OF THIS PAGE (When Data Entered)

REPORT DOCUMENTATION PAGE	READ INSTRUCTIONS BEFORE COMPLETING FORM
1. REPORT NUMBER: N00014-82-C-0144	2. GOVT ACCESSION NO.: AD-A117901
3. RECIPIENT'S CATALOG NUMBER:	
4. TITLE (and Subtitle): ULTRASONIC MEASUREMENT OF CASE DEPTH IN CASE HARDENED STEELS, Evaluation of Feasibility for the Ultrasonic Measurement of Case Depth in Case Hardened Steels	5. TYPE OF REPORT & PERIOD COVERED: FINAL REPORT 0001AD Jan - June 1982
	6. PERFORMING ORG. REPORT NUMBER:
7. AUTHOR(s): Morris S. Good	8. CONTRACT OR GRANT NUMBER(s): N00014-82-C-0144
9. PERFORMING ORGANIZATION NAME AND ADDRESS: Ultrasonics International, Inc. Three Neshaminy Interplex, Suite 215 Trevose, Penna. 19047	10. PROGRAM ELEMENT, PROJECT, TASK AREA & WORK UNIT NUMBERS:
11. CONTROLLING OFFICE NAME AND ADDRESS: David K. Beck, Contracting Officer Department of the Navy, ONR Arlington, Virginia 22217	12. REPORT DATE: July 1982 13. NUMBER OF PAGES: 53
14. MONITORING AGENCY NAME & ADDRESS(if different from Controlling Office): Dr. J. Goff Naval Surface Weapons Center White Oak Silver Spring, Maryland 20910	15. SECURITY CLASS. (of this report): Unclassified 15a. DECLASSIFICATION/DOWNGRADING SCHEDULE

16. DISTRIBUTION STATEMENT (of this Report)

Unlimited distribution: Public release is authorized.

17. DISTRIBUTION STATEMENT (of the abstract entered in Block 20, if different from Report)

18. SUPPLEMENTARY NOTES

19. KEY WORDS (Continue on reverse side if necessary and identify by block number)

ULTRASONIC ANGULATION PULSE-ECHO	RF SIGNAL AVERAGING
EFFECTIVE CASE DEPTH	SHEAR WAVE
CASE HARDENING	RAYLEIGH SCATTERING
SIGNAL PROCESSING	SPATIAL AVERAGING
	HILBERT TRANSFORMATION

20. ABSTRACT (Continue on reverse side if necessary and identify by block number)

To date, various methods have been proposed for measuring case depth in case hardened steels. Each method as described in past literature is restricted in practical application due to problems in area localization, geometry, sensitivity, compositional variations of different steels, and compositional changes due to carbon and/or nitrogen gradients formed during the hardening process.

DD FORM 1 JAN 73 1473 EDITION OF 1 NOV 65 IS OBSOLETE

Unclassified
SECURITY CLASSIFICATION OF THIS PAGE (When Data Entered)

Unclassified
SECURITY CLASSIFICATION OF THIS PAGE(When Data Entered)

Ultrasonic pulse-echo angulation is thought to have an inherent advantage over these other methods such as eddy current and magnetic permeability.

Prior restrictions of ultrasonically determining effective case depth were due to resolution problems caused by the extremely low signal-to-noise ratio and the apparent obscuring effect of the front surface echo. This study shows that with improved signal processing techniques such as RF signal averaging, enveloping, spatial averaging and smoothing, many of these prior restrictions can be relaxed, particularly regarding the measurement of case depths less than 2mm. Emphasis was placed on forming an algorithm via an ultrasonic angulation pulse-echo system, whereby effective case depths of .91mm, 1.40mm, and 1.98mm were analyzed. The algorithm measured these values as .94mm, 1.40mm, and 2.11mm with respective standard deviations of .25mm, .23mm and .81mm respectively.

Feasibility for development of an ultrasonic device for measuring effective case depth in case hardened steels has been shown. This is due to the added range of case depths that ultrasonics can measure, area localization, relatively insignificant signal distortion due to depth, relative stability regarding material composition, and especially the potential for further technique refinement.

TABLE OF CONTENTS

LIST OF FIGURES

LIST OF FIGURES (cont'd)

LIST OF TABLES

INTRODUCTION

Our goal is to nondestructively determine effective case depth via an ultrasonic procedure. Characteristics which would be desirable for a case depth meter are measurement localization to a well defined area, effectiveness over a large range of case depth values, consistent accuracy, and application to the wide range of steels in which case hardening is performed. A technique thought to have such characteristics is the ultrasonic pulse-echo angulation method.

As reported by Emerson {1} three basic nondestructive methods exist for measuring case depth; ultrasound, eddy current, and magnetic permeability. Each method has advantages and restrictions which make one technique more pragmatic than another under a given test criteria and environment. The dominant parameters affecting the selection of a given methodology over another is the inherent sensitivity restrictions characteristic of a given technique for a specific case depth, Table 1.

Regarding the ultrasonic pulse-echo technique, area localization is determined by sonic resolution, approximately 1mm or .04 inch, the range of case depths which this method may be effective is approximately .01 inch and greater. This range reflects an extension of angulation methods previously reported, Table 1. The accuracy restrictions of the technique are related to the uncertainty involving leading edge detection of the Rayleigh back scatter and the offset distance between the desired effective case depth and the back scatter leading edge. The difficulty has been the extremely low signal-to-noise ratio due to the inherent low signal amplitude of the back scatter response. By means of signal averaging and spatial averaging an extreme amount of progress has been made concerning the implementation of this method as a quality control tool.

The accurate and consistent measurement of effective case depth is a vital concern being that insufficient case depth would indicate an article not able to meet specified wear constraints while an excessively large case depth could facilitate a fracture due to increased brittleness of the hardened zone. Case depth can vary considerably from piece to piece within a signal batch of articles and even from point to point on a given article. Four significant parameters affecting case depth are solid carburizing material distribution, temperature distribution, quenching, and material removal by either grinding or machining {4}.

In discussing case depth, two definitions must be clarified, total case depth and effective case depth. Total case depth represents the surface depth to which the parent core material is affected by the case hardening procedure. Effective case depth represents the surface depth to which a specified hardness is achieved. Most material specifications give an effective case depth and a hardness value to which effective case depth is measured.

TABLE 1. CASE DEPTH MEASUREMENT CHARACTERISTICS OF ULTRASOUND, EDDY CURRENT AND MAGNETIC PERMEABILIT

TECHNIQUE	REPORTED RANGES OF USE	GENERAL DISCUSSION
ULTRASOUND		
Pulse Echo		
Normal Beam	.39 inch, 10mm Smallest Reported Value {1}. 3.4 inch, 80mm Largest Reported Value {1}. Reported study performed in iron.	Small case depth measurement is limited by resolution of case/core interface echo and front surface echo {1} . Technique should be accurate in measuring larger case depths. Detection of case/core interface echo becomes difficult when transition from case to core material is not markedly pronounced.
Angulation	.08 inch, 2mm Smallest Reported Value {2}. .59 inch, 15mm Largest Reported Value {1}. Reported study performed in steel.	Small case depth measurement limited by resolution of Rayleigh back scatter and the front surface echo. Technique should be accurate in measuring larger case depths and be more effective than normal beam when hardness gradient is not markedly pronounced. Frequency selection is critical for providing significantly different scattering characteristics of case and core material.
Goniometry	.08 inch, 2mm Largest Reported Value {2}. Reported study performed in steel.	Technique is useful in hardening depths of approximately 2mm and less {2}. The technique requires first, extreme precision and sensitivity which increases system expense and secondly, an extended planar surface which causes localization problems {2}. Conceptually, the technique is dependent on wave velocity differences between the case and core material and is not pragmatic in steels where wave velocity changes are not significant {1}.
EDDY CURRENT	.03 inch, .8mm Smallest Reported Value {3}. .12 inch 3.0mm Largest Reported Value {1}. Reported study performed in steel.	Technique is sensitive to case depths less than 3mm and the penetration is dependent on the alternating frequency used; 50 Hz for 1mm and 5 Hz for 3mm {1}.

TABLE 1. CASE DEPTH MEASUREMENT CHARACTERISTICS OF ULTRASOUND, EDDY CURRENT AND MAGNETIC PERMEABILITY (cor

TECHNIQUE	REPORTED RANGES OF USE	GENERAL DISCUSSION
		Interfering parameters such as changes in steel composition (particularly carbon), physical changes, dimensional changes, and surface stresses and strains can cause significant measurement fluctuations {3}. Inherently eddy current is more sensitive to anterior changes and, therefore, becomes increasingly less sensitive with depth. A maximum of 3mm penetration under good conditions is estimated as a limiting value {1}.
MAGNETIC PERMEABILITY	.08 inch, 2mm Smallest Reported Value {1}. .39 inch, 10mm Largest Reported Value {1}. Reported study performed in bar steel.	Interfering factors such as compositional changes and consistent magnetic coupling cause significant measurement fluctuations {1}.

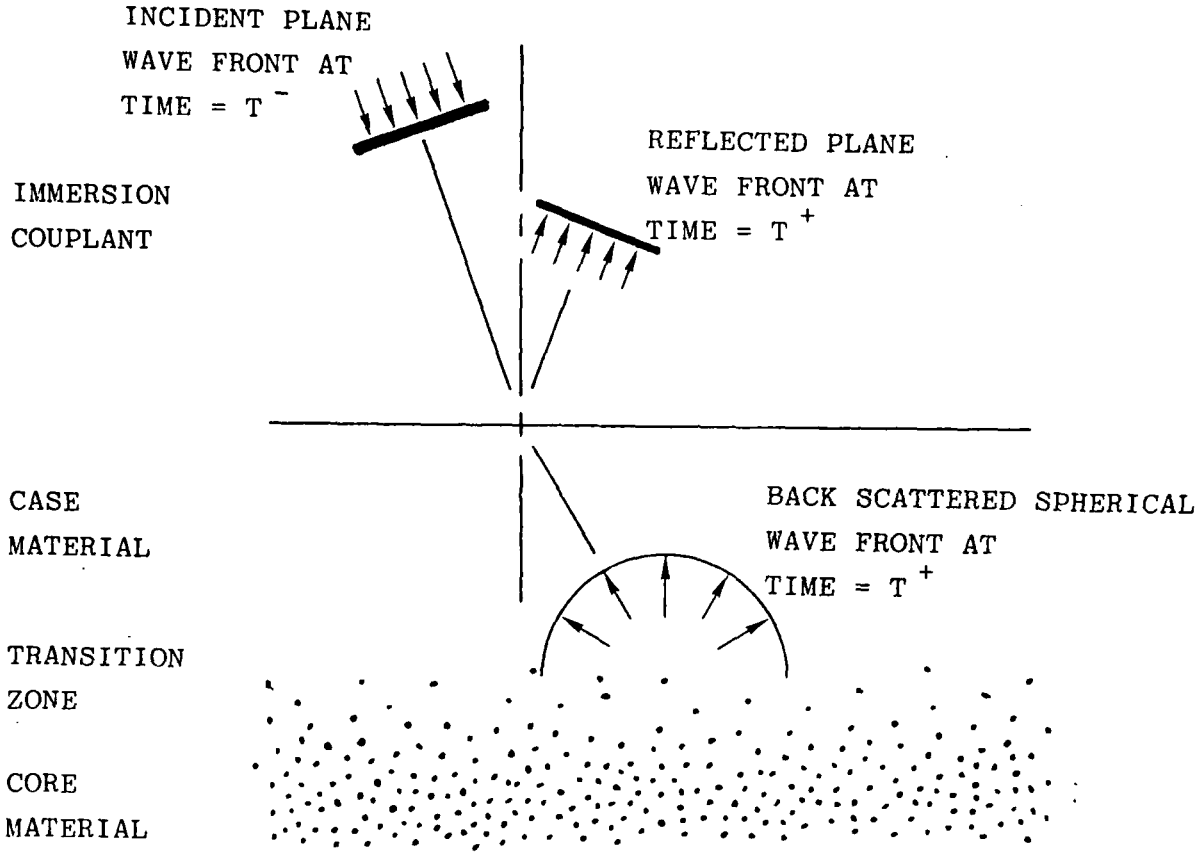

Figure 1. Incident, Reflected, Refracted, and Back Scattered Wave Phenomena Resulting From Case Hardened Specimen Interaction

Our first goal was to refine a technique such that the signal-to-noise ratio was sufficiently large to provide consistent measurements and second, to relate effective case depth to the depth at which the back scattered energy originated.

TECHNIQUES EVALUATED FOR OPTIMAL DATA ACQUISITION

Several ultrasonic techniques were evaluated for their respective effectiveness in terms of signal-to-noise ratio. Techniques that were evaluated included normal beam pulse-echo via immersion and beam angulation pulse-echo via immersion in both the refracted longitudinal mode and the refracted shear mode. To further enhance data acquisition high energy pulsers, computer interfaced systems, and electronic shielding devices were also considered.

Consider the technique illustrated in Figure 1. A longitudinal wave is impingent on a water/steel interface at a known incident angle. When the incident angle equals zero we have the trivial case of normal incidence. As the incident angle is increased, back scattered signal amplitudes can be monitored. Given case depth measurements, time ranges can be established where back scattered signals are anticipated. Angulation techniques suggested by Perennes, Jussiaume, and Gaillot {2} and Flambard and Lambert {5} direct the reflected wave front away from the transducer. This action is two-fold in function. First, the front wall surface echo returning to the transducer is a portion of the spherical wave pattern and, therefore, the energy levels are smaller than the reflected plane wave front by several orders of magnitude. This reduces the masking effect of the front wall echo on superficial scatters. Second, the incident angle is such to cultivate the back scattered signal. Goelbels {6} examined the tradeoffs between using shear waves over longitudinal waves and documented that the relative difference between back scattered energy of shear to longitudinal mode of vibration is a factor of approximately 45 or 33 dB.

Prior to discussing data acquisition and signal analysis, let us first discuss the preparation and various material characteristics of the case hardened specimen.

CASE HARDENED SPECIMEN, PREPARATION AND MATERIAL CHARACTERISTICS

A block of 1060 steel having a rectangular cross-section of dimensions 2.5 cm by 2.5 cm, 1.0 inch by 1.0 inch, and a length of 10.2 cm, 4.0 inch, was induction hardened such that a planar case depth of 2. mm, .08 inch, existed. Induction hardening processes were used to prevent surface composition changes associated with diffusing additional carbon into the surface layer.

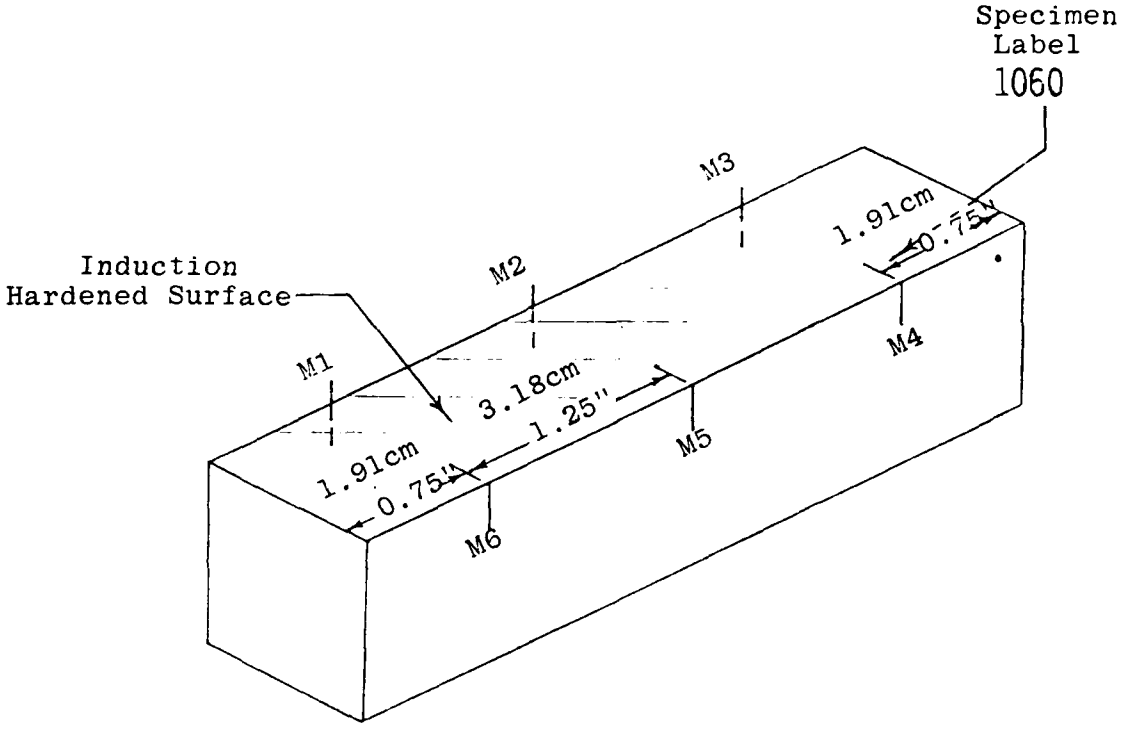

M = Line Along Which Hardness was Measured

Figure 2. Case Hardened Specimen with Indications M1 through M6 Displaying Position of Microhardness Traverses

Microtransverse hardness profiles via a Knoop microhardness indentor were acquired along six marked indications, Figure 2. Transverse hardness profiles corresponding to each marked indication are illustrated in Figures 3 and 4. A surface hardness of 54, Rockwell scale C, was obtained with a smooth transition to the softer core material.

For the particular specimen considered a hardness value of 30, Rockwell scale C, was selected as the effective case depth specification value. Nominal case depth at three points were measured. These measurements were determined as the average between the case depths measured respectively along the lines M3-M4, M2-M5, and M1-M6, Table 2.

TABLE 2. CASE DEPTH MEASUREMENTS OF 1060 STEEL SPECIMEN, RAW FINISH

LINE	EFFECTIVE CASE DEPTH					
	LEFT POINT		RIGHT POINT		AVERAGE LINE VALUE	
M3-M4	M3:	2.2mm, .085"	M4:	2.1mm, .083"	2.1mm, .084"	
M2-M5	M2:	1.7mm, .076"	M5:	1.5mm, .058"	1.7mm, .067"	
M1-M6	M1:	0.6mm, .024"	M6:	2.6mm, .104"	1.6mm, .064"	

Micrographs were acquired of the case, transition zone, and core areas, Figure 5. Each micrograph represents a 500X magnification. The left micrograph is characteristic of a nearly 100% martensite. The fine intergranular structure forms the bulk of the hardened region. The center micrograph displays the transition between a predominately martensitic structure to a predominately pearlitic structure. The pearlite is characterized by alternating laminates of cementite and ferrite. The interlaminar spacing between these layers becomes more coarse as depth increases. The right micrograph illustrates a predominately pearlitic structure. Note the diamond impressions resulting after a Knoop hardness test at various depth indications. The difference in ultrasonic scattering properties are thought to be related to these changes within the internal grain structure.

A tapered wedge can be removed from the case surface by grinding. If .76mm or .030" are removed from the unlabeled edge, the average line effective case depth measurements are 1.98mm, .078"; 1.40mm, .055"; and .91mm, .036" for lines M3-M4, M2-M5, and M1-M6 respectively, Figure 6.

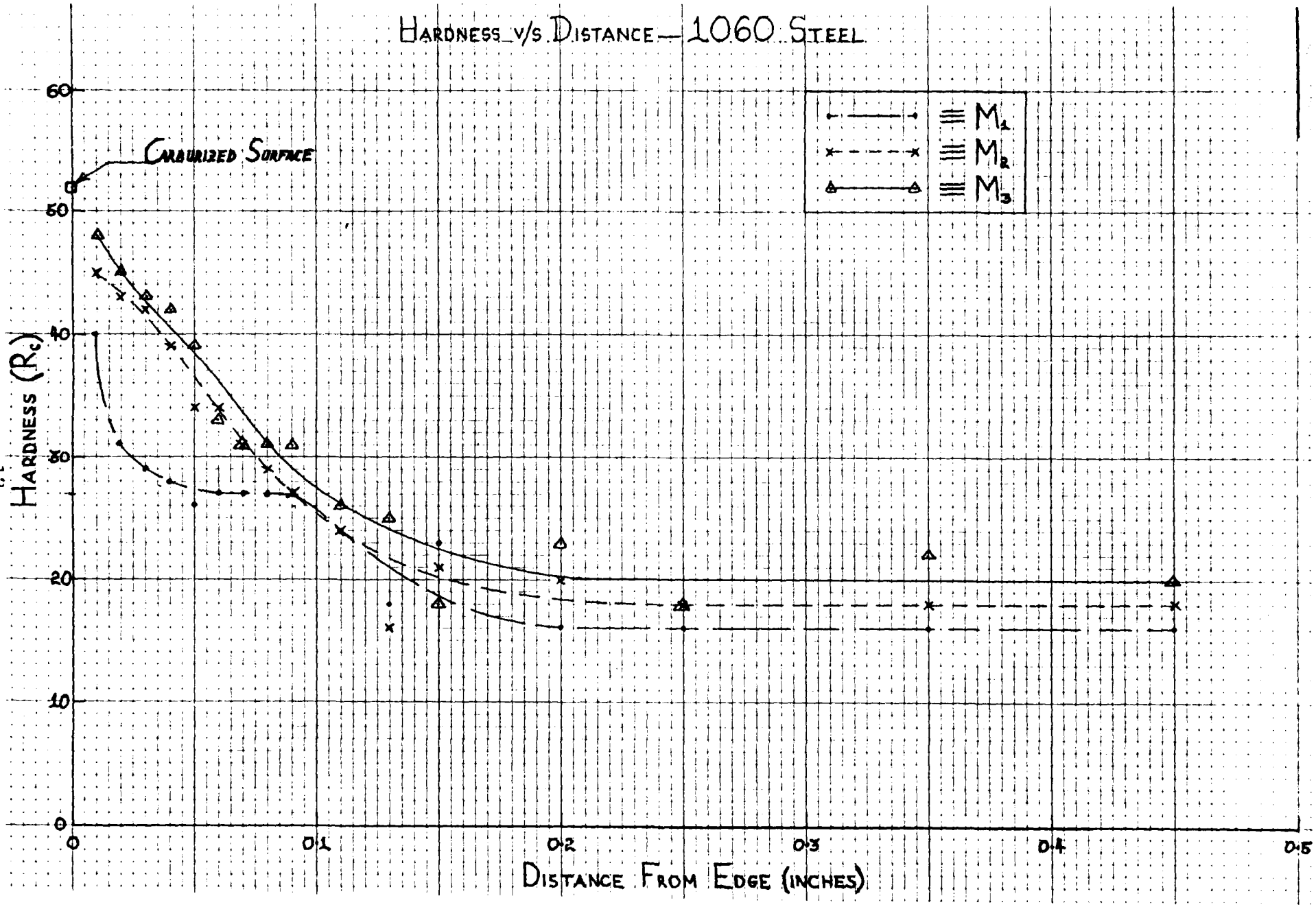

Figure 3. Transverse Microhardness Profiles Along M1, M2, and M3

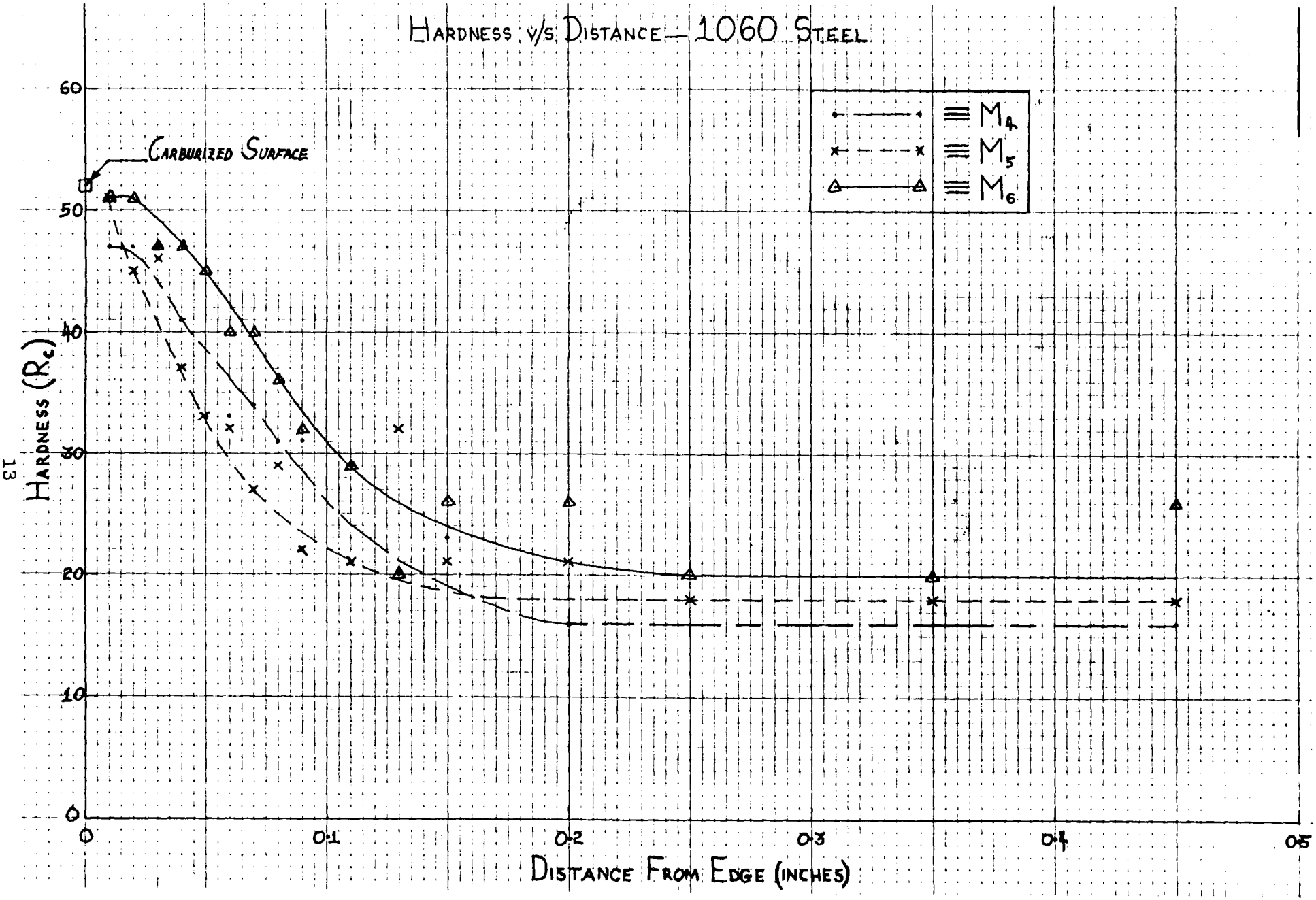

Figure 4 Transverse Microhardness Profiles Al

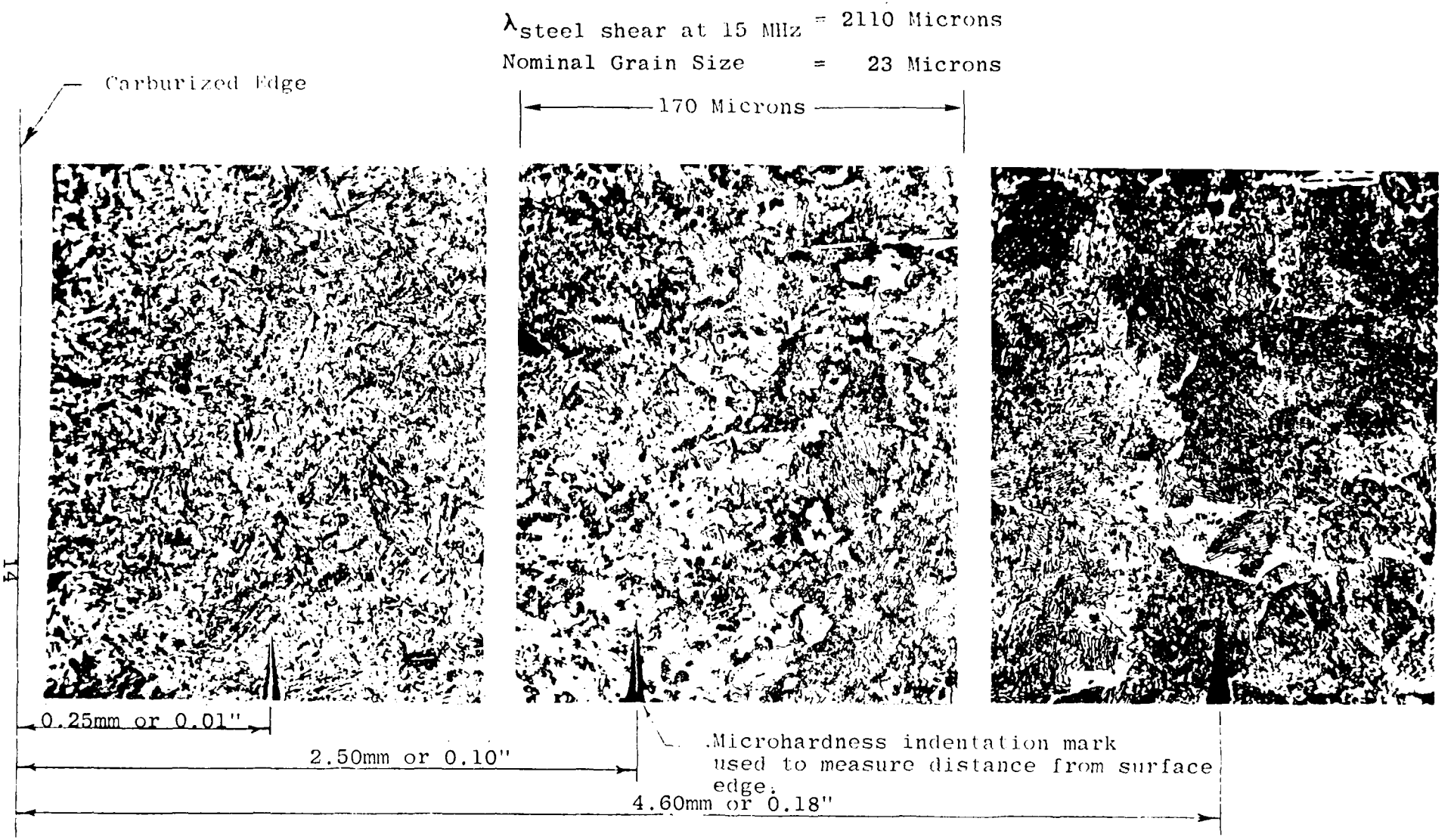

a. Case Region, Martensitic Structure

b. Transition Zone, Martensitic to Pearlite Structure

c. Core Region, Pealite Structure

Figure 5. Micrographs of 1060 Steel Specimen at 500X Magnification, Nital Etching

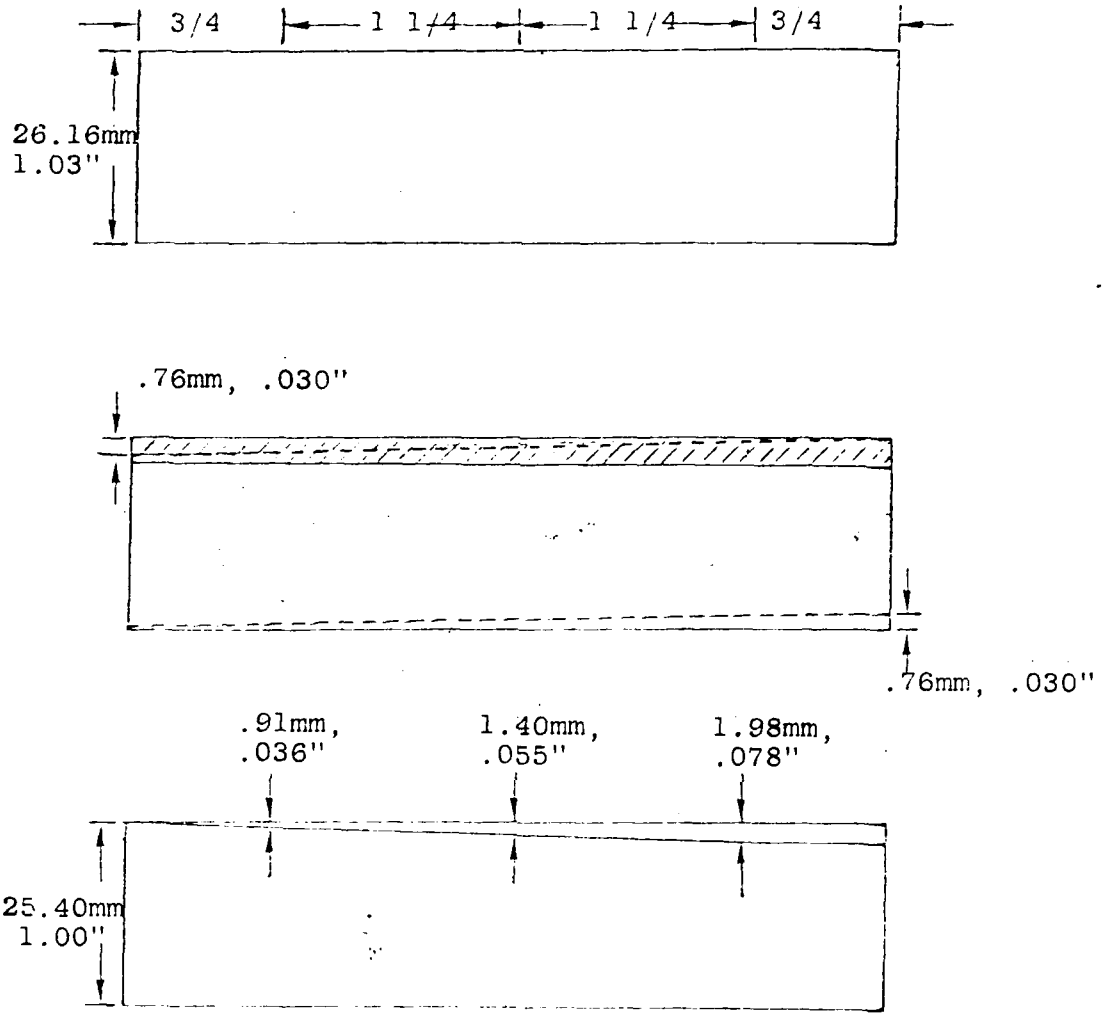

Figure 6. Preparation of 1060 Steel Specimen for Variable Case Hardened Depth

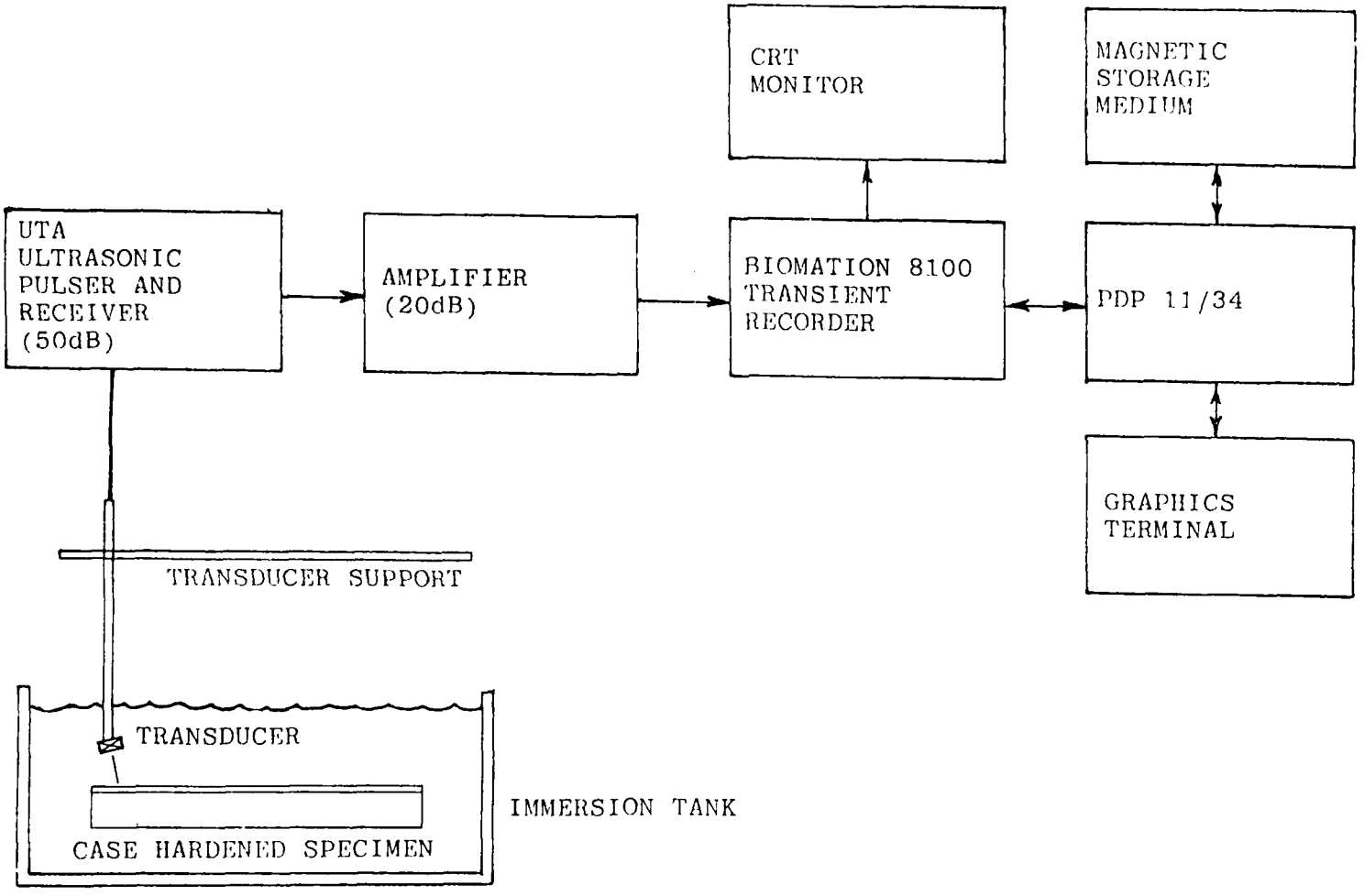

Figure 7. Block Diagram of Computer Controlled Data Acquisition and Analysis System

DATA ACQUISITION

A block diagram of the computer controlled data acquisition and analysis system appears in Figure 7. Contained within the system is a UTA ultrasonic pulser and receiver, a fixed gain RF amplifier, a Biomation 8100 transient recorder, a PDP 11/34 minicomputer, and other peripheral equipment such as a CRT monitor, a magnetic storage device and a graphics terminal. An optimized protocol was developed via this system for enhanced data acquisition. This resulted from the accumulative effect of a series of ministudies to evaluate various techniques that would be contained within the data acquisition protocol. The ministudies included RF signal averaging to reduce noise levels and transducer angulation to determine optimum system sensitivity towards the combined effects of sonofication, scattering, and reception of back scattered signals from the core material. Other phenomena discussed are obscuring effects of lateral beam resolution, beam side lobes and surface roughness.

Signal Averaging

Signal averaging was used to reduce noise levels to acceptable levels. Progress in this area can greatly simplify further analysis and increase system consistency. As illustrated in Figure 8, a single RF transient response is characteristic of a signal-to-noise ratio of approximately one-third. Since spurious RF spurts occurred randomly, their effects could be minimized through signal averaging techniques. Normally an averaged response of 8 signals provides sufficient noise reduction, Figure 9. However, since the spurious signals are approximately 3 times larger than the Rayleigh back scatter, averaging of 255 times proved useful, Figure 10. Note the noise reduction corresponding to the case layer between the 8 and the 255 times averaged signal. This is significant since the accurate determination of case depth is dependent on clear separation of the two regions, low versus high amplitude back scatter.

Transducer Selection

A variety of immersion transducers were used to determine optimal transducer characteristics for data acquisition and analysis, Figures 11-16. Primary concerns were sensitivity to receiving back scatter responses, axial resolution relative to the separation of low versus high back scatter regions, and the obfuscation of the surface echo with the interaction of the side lobe energy reflected from the case specimen surface. Table 3 itemizes several transducers according to their characteristics and lists comments relating to their desirability.

Transducer F05008 was selected due to the relative amplitude difference between values of the back scattered signals resulting from the case and core regions, the sharp transition between the two forms of back scattered energy, and the insignificant level

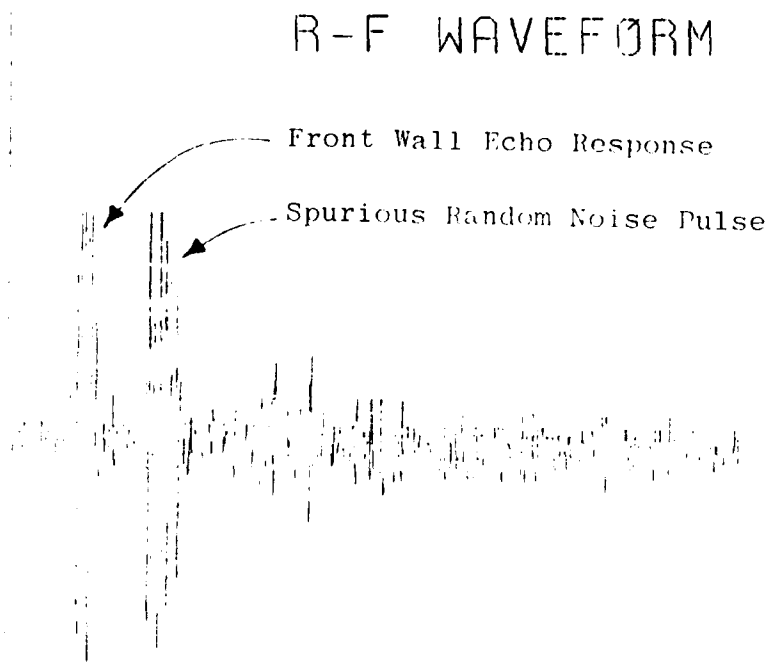

Figure 8. Case Hardened Signal Response, Averaged 001 Times

Figure 9. Case Hardened Signal Response, Averaged 008 Times

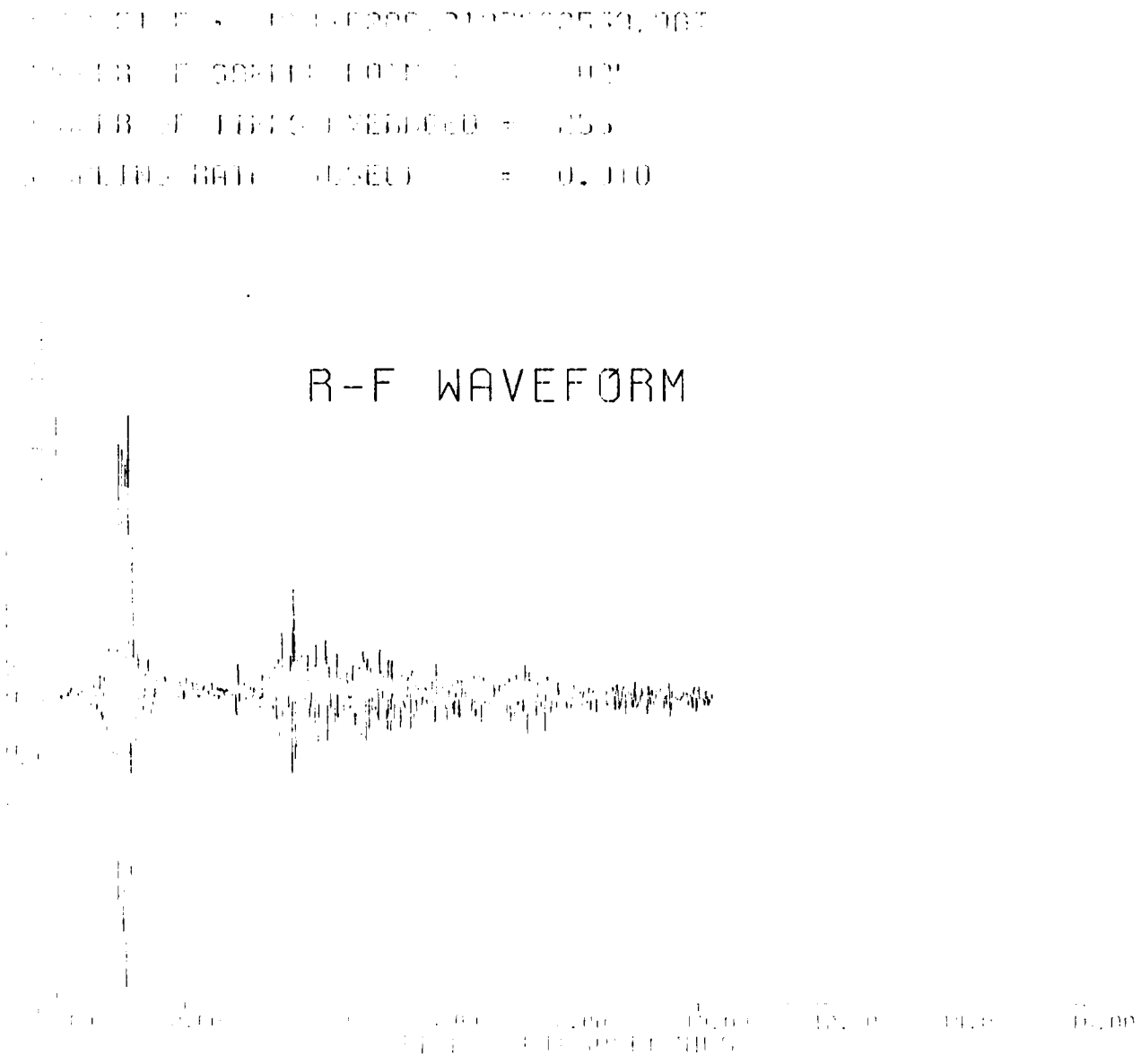

Figure 10. Case Hardened Signal Response, Averaged 255 Times

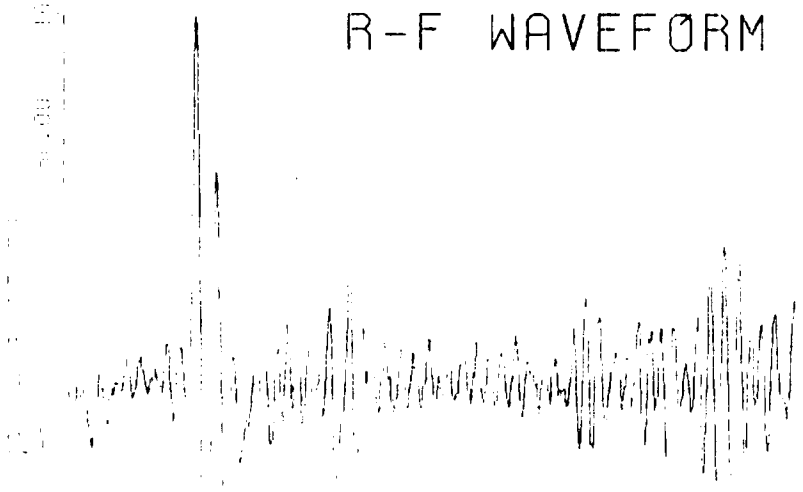

Transducer Characteristics:

Frequency - 5 MHz
Focal Depth - 1.3 Inch Near Field Value
Crystal Dia. - .25 Inches

Figure 11. Ultrasonic Response of Case Hardened Specimen Using Transducer A18824

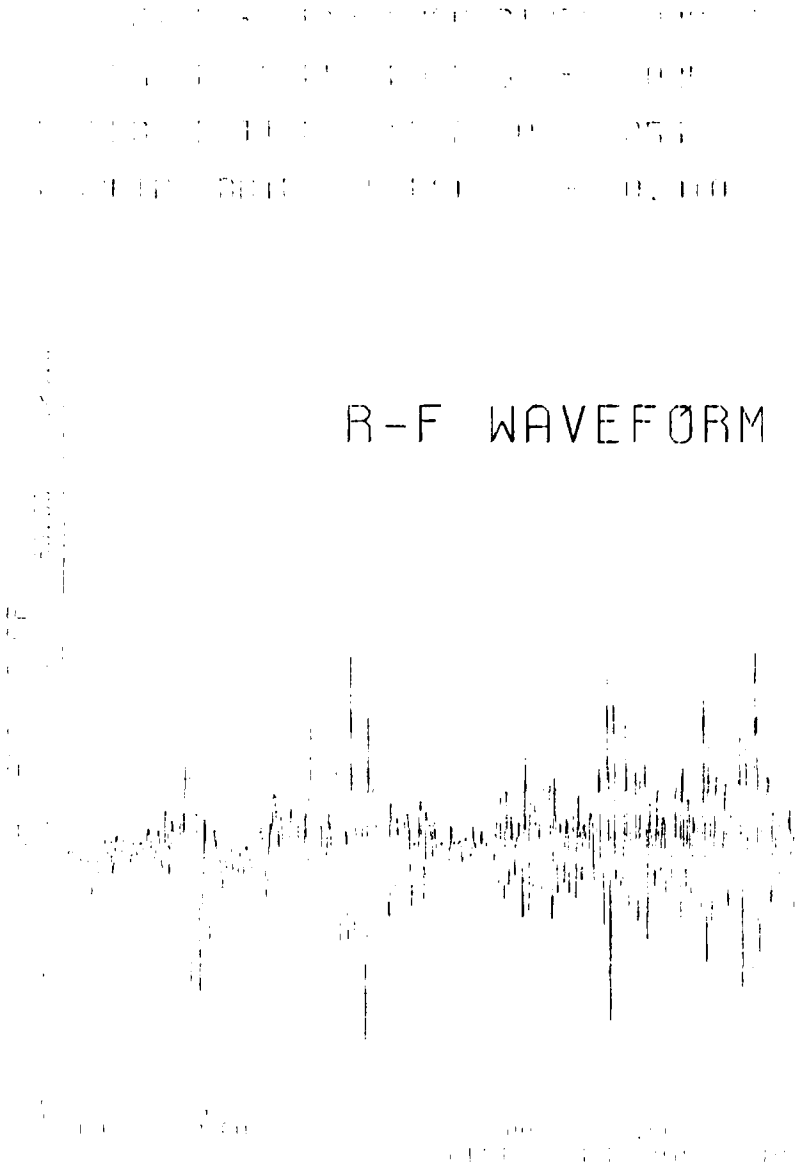

Transducer Characteristics:

Frequency - 10 MHz, Broadbanded
Focal Depth - 2.7 Inch Near Field Value
Crystal Diameter - .25 Inches

Figure 12. Ultrasonic Response of Case Hardened Specimen Using Transducer C28028

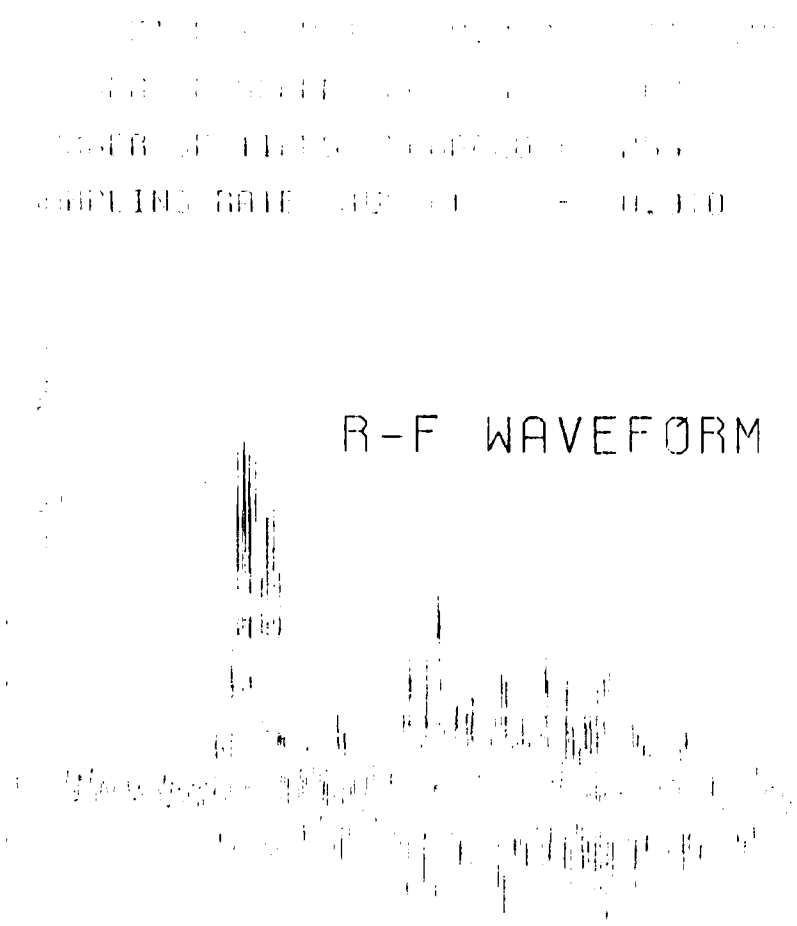

Trausducer Characteristics:

Frequency - 10 MHz, Broadbanded
Focal Depth - 1.5 Inch Focus
Crystal Dia. - .50 Inches

Figure 13. Ultrasonic Response of Case Hardened Specimen Using Transducer G15113

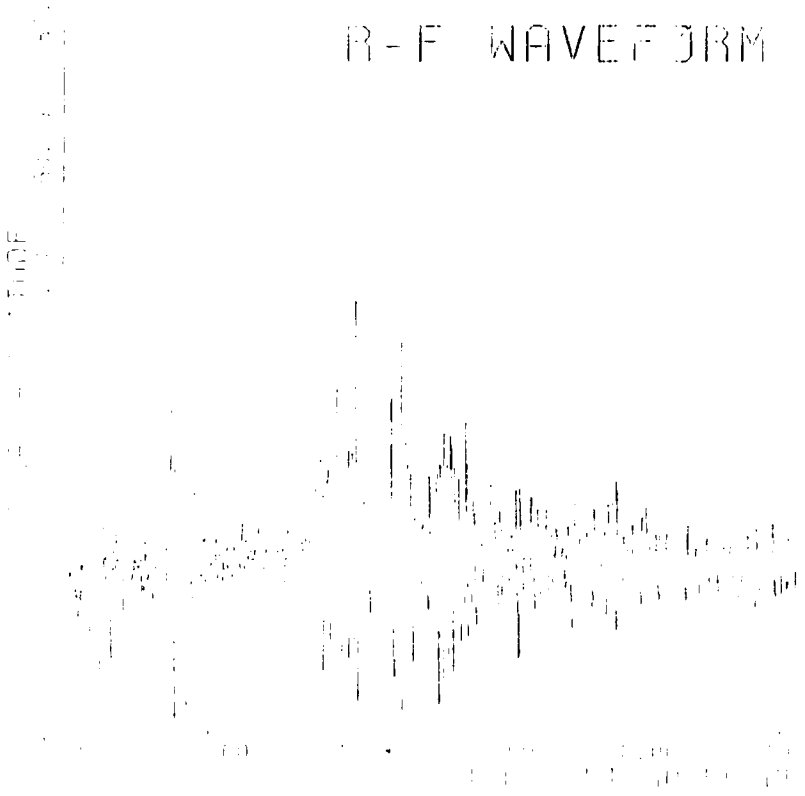

Transducer Characteristics:

Frequency - 20 MHz, Broadbanded
Focal Depth - 1.25 Inch Focus
Crystal Dia. - .25 Inches

Figure 14. Ultrasonic Response of Case Hardened Specimen Using Transducer K20822

Transducer Characteristics:

Frequency - 25 MHz, Broadbanded
Focal Depth - 1.5 Inch Focus
Crystal Dia. - .25 Inches

Figure 15. Ultrasonic Response of Case Hardened Specimen Using Transducer B11728

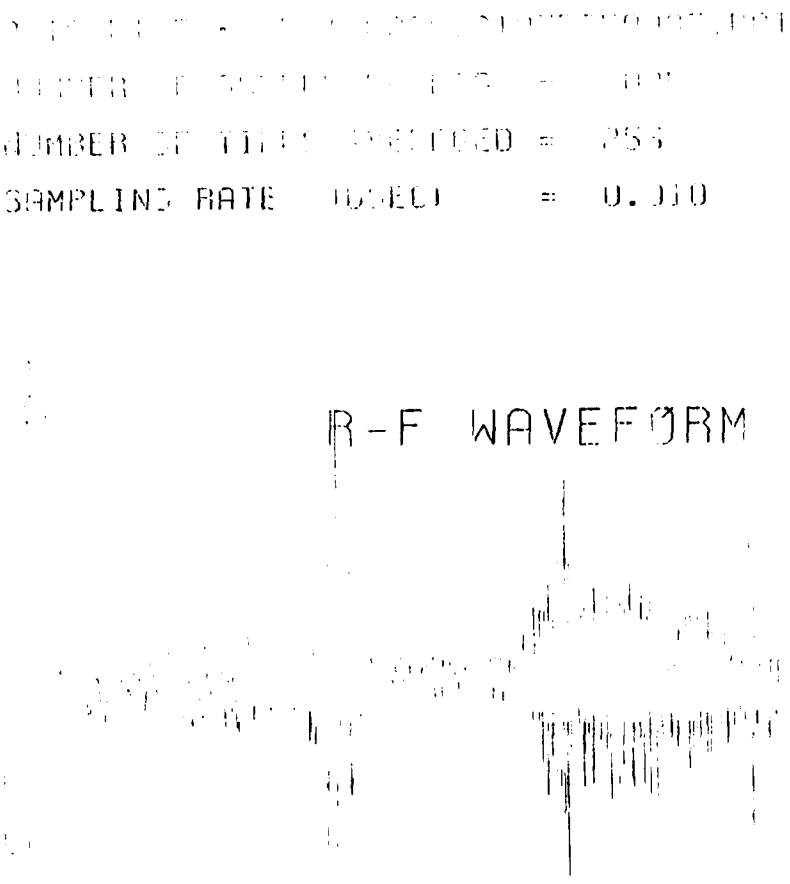

Transducer Characteristics:

Frequency - 15 MHz, Broadbanded
Focal Depth - 1.5 Inch Focus
Crystal Dia. - .25 Inches

Figure 16. Ultrasonic Response of Case Hardened Specimen Using Transducer F05008

of side lobe energy. The lack of sharpness regarding the transition between the case and core region may be attributed to lateral beam resolution. Due to a transducer angulation of 20^{o} in water the refracted shear wave lateral resolution has a projected component which affects the resolution of the case and core areas. Transducers of high lateral beam resolution are critical to forming a sharp distinction between the two areas. Figure 17 illustrates the effects of lateral resolution. For the remainder of the study transducer F05008 was used exclusively.

TABLE 3. ULTRASONIC TRANSDUCER EVALUATION REGARDING CASE DEPTH MEASUREMENT

Transducer				Case/Core Separation	Side Lobe Energy
No.	Dia.	F*	Focal Depth		
A18824	.25"	5	1.3"	Case/Core transition not easily resolved	Significant presence
C28028	.25"	10	2.7"	Case/Core transition not easily resolved	Significant presence
G15118	.50"	10	1.5"	Case/Core transition not easily resolved	Not observed
K20822	.25"	20	1.3"	Case/Core transition easily resolved	Significant presence
B11728	.25"	25	1.5"	Case/Core relative amplitude significantly different	Not observed
F05008	.25"	15	1.5"	Case/Core transition easily resolved	Insignificant presence

*Values given in units of MHz

Transducer Angulation

Sonic beam angulation enables us to selectively use refracted longitudinal or shear waves. As reported by Perennes, Jessiaume, and Gaillot {2}, and Flambard and Lambert {5} an inclination angle of 20^{o} in water, 45^{o} in hardened steel, was used. Goelbels {6} in his discussions concerning ultrasonic grain size measurement elaborates that the relative amplitude difference between shear and longitudinal back scattered energy in steel is approximately a factor of 45 or 33 dB. Frequency values for each vibration mode were selected such that the wave lengths of the two respective vibration modes were set equal. Since the back

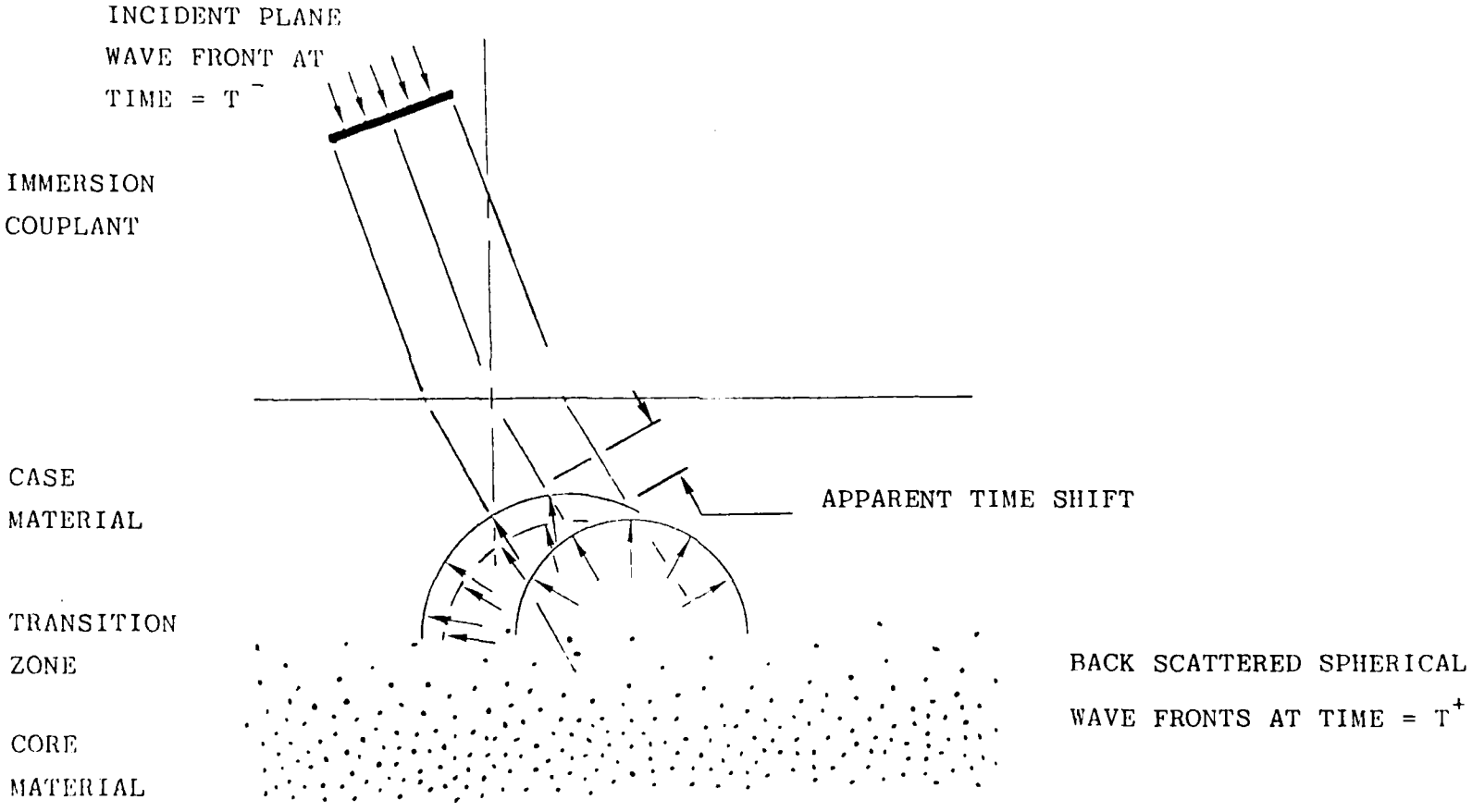

Figure 17. Affects of Lateral Beam Resolution and Divergence on Apparent Back Scatter Arrival Time

scattered signals are extremely small, shear wave excitation would seem the only logical choice until a system incorporating high energy pulsers, more efficient transducers in both send and receive, better electronic shielding, and greater signal amplification allow longitudinal wave back scatter to have a realistic signal-to-noise ratio.

To form a complete study, back scattered amplitude values were recorded at selected degree inclinations from 0^{o} through 30^{o}, in water. A graph of recorded amplitude values versus inclination angle, Figure 18, showed 19^{o} and 20^{o} as optimal inclination angles. A more detailed analysis indicates that three independent wave phenomena effect the received amplitude values due to angulation alone. They are percentage of mode conversion of the incident wave to a refracted shear wave, resolution dependency on transducer lateral and axial resolution restrictions, and lateral displacement offset of back scattered spherical wave fronts, Figure 19. The predominant effect in this study is attributed towards the percentage of mode conversion. Since the case depths are relatively small compared to transducer diameter, lateral offsets were thought to have an insignificant effect. Signal amplitude values corresponding to angles 0^{o} through 14^{o} were not graphed since signal amplitude values could not be isolated.

Surface Roughness

Past work efforts attempt to measure case depth by an extension of using pulse-echo techniques such as

$$d = V_{ss} \left(\frac{T_{bs} - T_{fs}}{2}\right) \cos\left[\text{Arcsin}\left(\frac{V_{ss}}{V_{wl}} \sin\theta\right)\right], \quad \text{Equation (1)}$$

where $d \equiv$ Case Depth

$\theta \equiv$ Inclination Angle, Water

$V_{wl} \equiv$ Wave Velocity, Water Longitudinal

$V_{ss} \equiv$ Wave Velocity Steel Shear

$T_{bs} \equiv$ Arrival Time, Back Scatter

$T_{fs} \equiv$ Arrival Time, Front Surface

An inherent foible contained within this approach is the accurate determination of T_{fs}. This is routinely performed in most pulse-echo situations. However, the water-to-steel interface echo response can vary significantly at a precision ground surface let alone a rough or raw machined surface, Figures 20 and 21. Since in practice a designed probe would be placed on the article surface to be evaluated the surface displacement could be included within a calibration procedure. The instrument wou d then assume that the probe would be placed on an article in a like fashion for all subsequent measurements. Truly the instability of the front wall echo could otherwise be a significant error source.

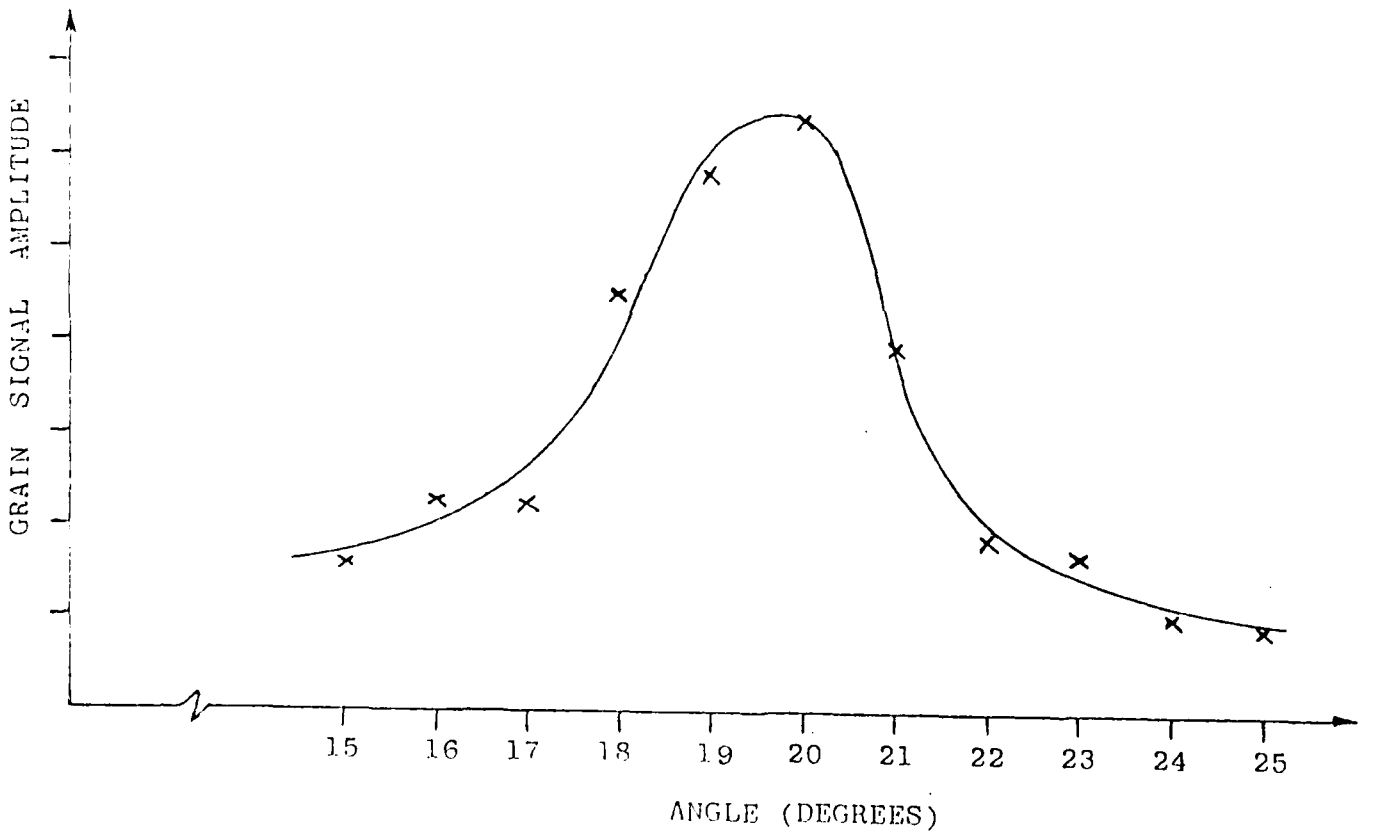

Figure 18. Shear Wave Back Scatter Amplitude Resulting From Interior Parent Grain Boundaries Versus Incident Angle

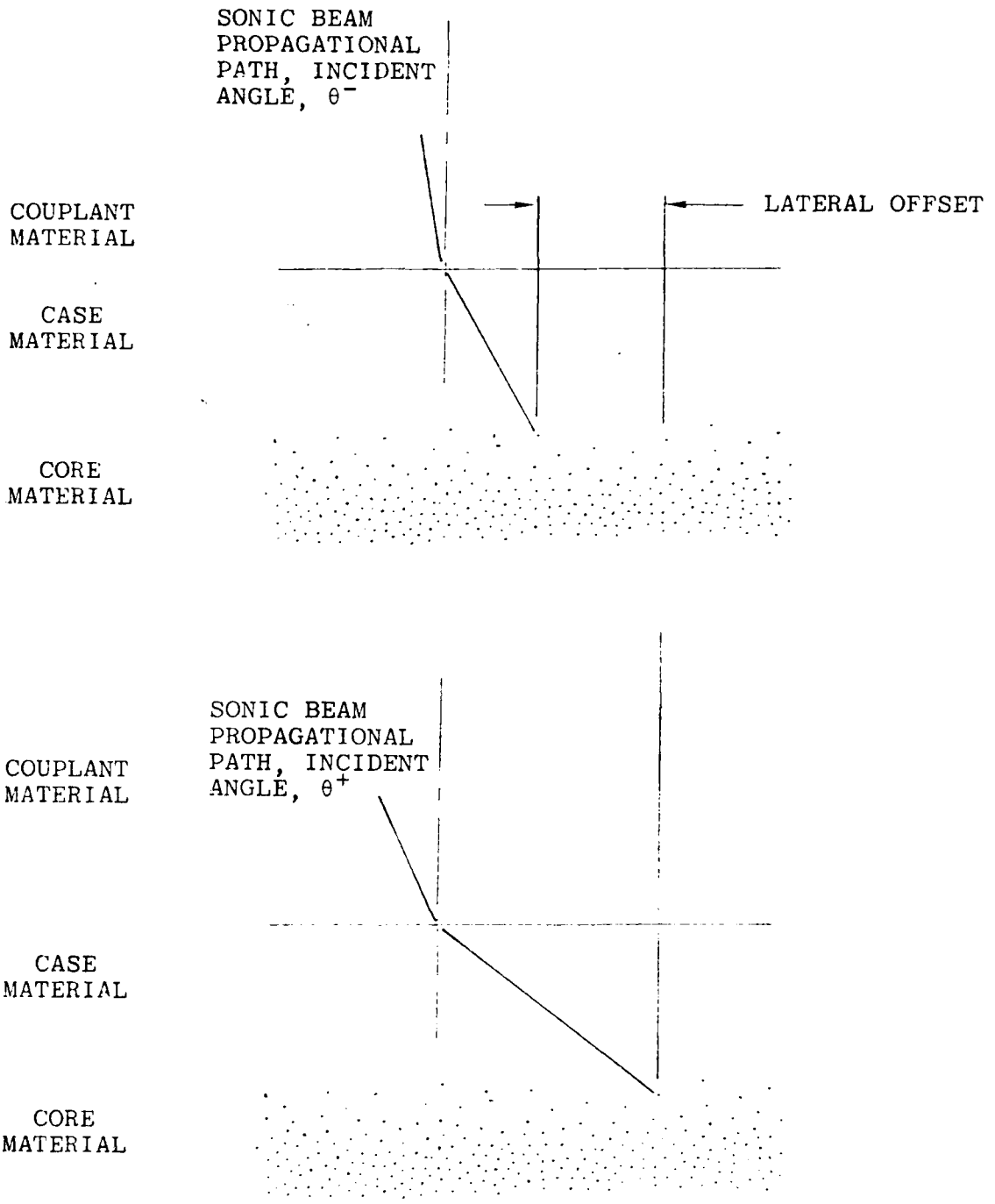

Figure 19. Lateral Offset Caused by Changes in Incident Angle, (Affects More Pronounced for Greater Case Depth)

DATA FILE : D:\I:F200.210\BOUGH.DAT
NUMBER OF SAMPLE POINTS = 1024
NUMBER OF TIMES AVERAGED = 255
SAMPLING RATE (USEC) = 0.010

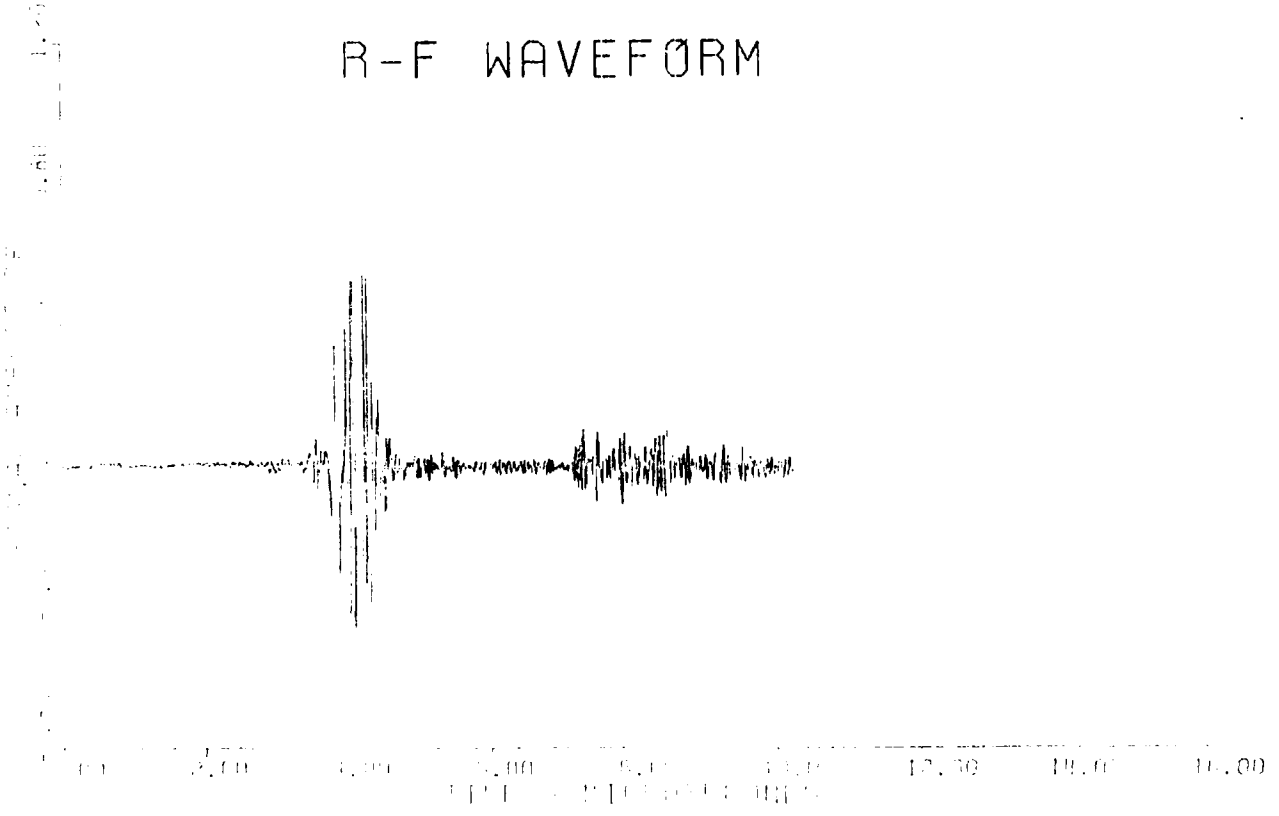

Figure 20. Surface Roughness Effect - Rough Surface Finish (Untreated)

DATA FILE : DY1:[200,210]SMOOTH
NUMBER OF SAMPLE POINTS = 1024
NUMBER OF TIMES AVERAGED = 255
SAMPLING RATE (USEC) = 0.010

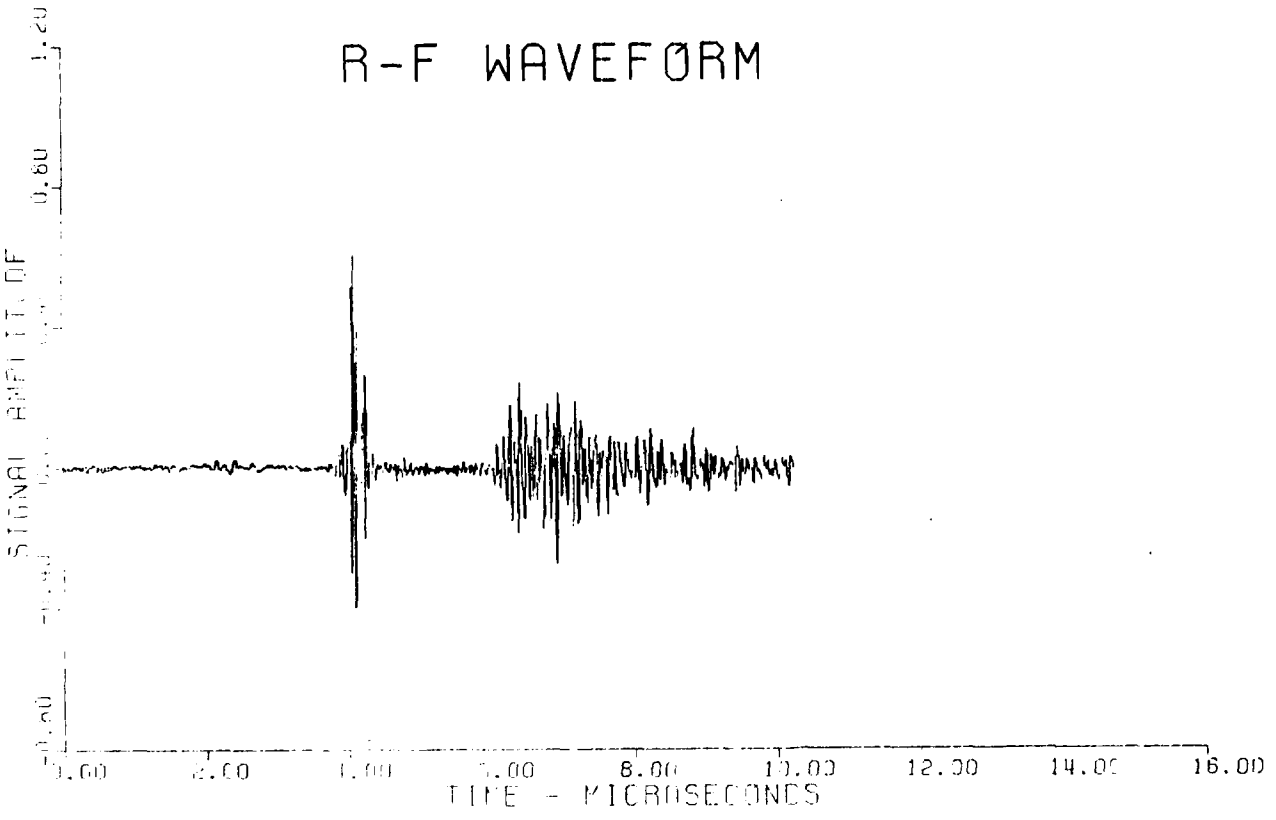

Figure 21. Surface Roughness Effect - Smooth Surface Finish (Ground)

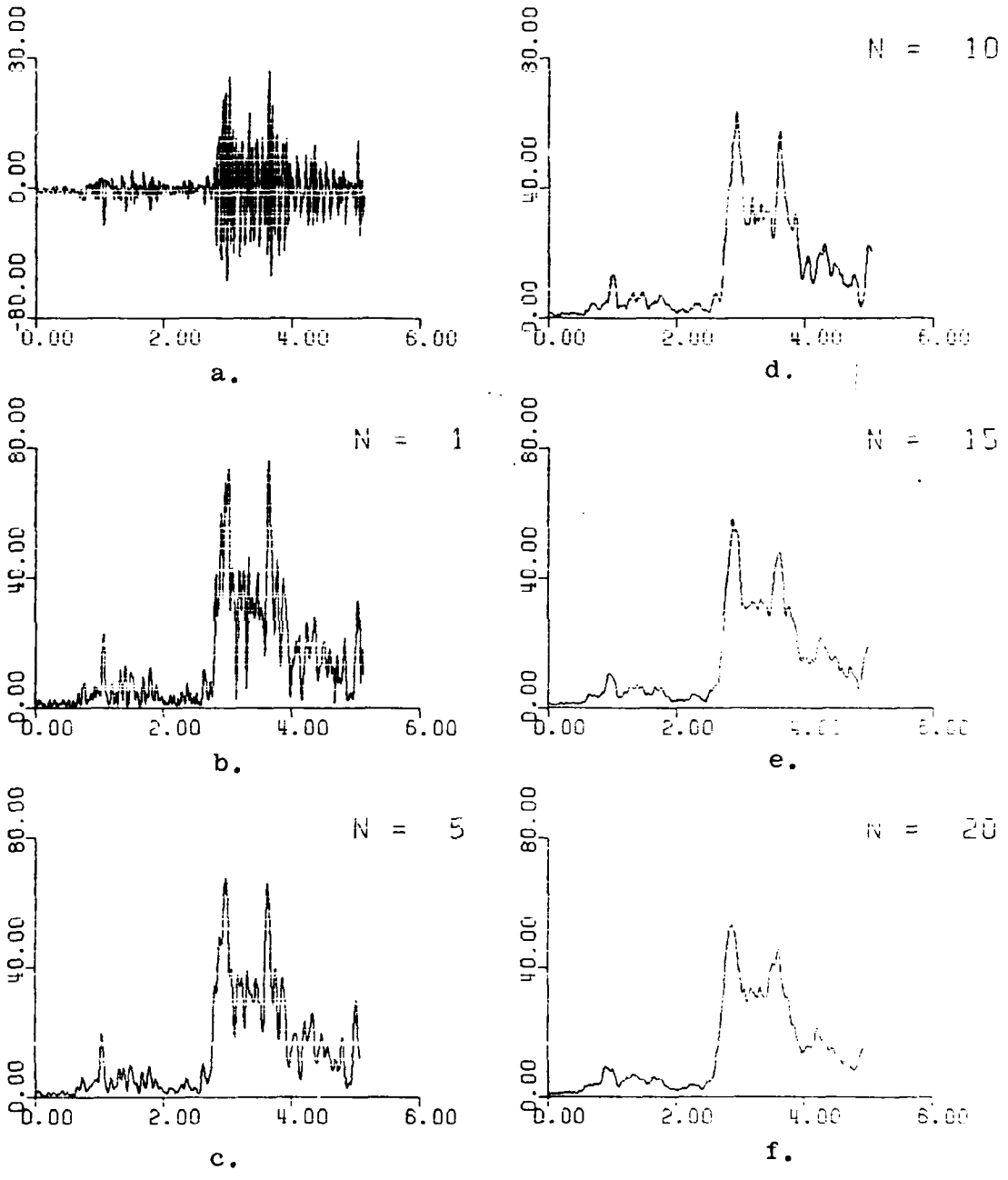

Figure 22. Signal Processing Involving Envelope Determination and Smoothing

a. RF Signal, 255 Times Averaged
b. Signal Envelope Via the Hilbert Transformation
c. Smoothed Envelope Using a .04 μ Second MAW
d. Smoothed Envelope Using a .09 μ Second MAW
e. Smoothed Envelope Using a .14 μ Second MAW
f. Smoothed Envelope Using a .19 μ Second MAW

SIGNAL ANALYSIS

In determining case depth three processes were accomplished sequentially. They were envelope determination via the Hilbert transform, spatial averaging of several stored envelopes, envelope smoothing using a Moving Average Window (MAW) and determining the beginning of the back scatter phenomena using a threshold criteria. To determine case depth it became extremely important to obtain an analysis procedure which could be repeated with acceptable accuracy. After acquiring an enhanced RF signal via singal averaging an envelope was determined by means of the Hilbert transform. However, the envelope underwent a significant change with the slightest displacement of the case hardened specimen {6}. To obtain back scattering characteristics of a material zone rather than a specific point spatial averaging of several envelopes, in effect from the same region, was performed.

Envelope Determination and Smoothing

Initially the RF signal envelope was determined, however, depression of an irregular and severe nature hindered the detection of the leading edge of the back scattered signal. A MAW of variable length was used to filter high frequency components from the envelope. These effects are illustrated in Figure 22. The trade off in using this technique is decreased resolution with an increased window size. Window sizes of .04, .09, .14, and .19 μ seconds, were used to establish trends.

Another problem developed with respect to what seemed periodic peaks and depressions in the smoothed envelope. Although these responses are valid and are repeatable at a particular point, they became a significant error source regarding consistency in back scatter leading edge detection. This resulted since the back scatter signal is extremely dependent on point location and that a lateral displacement of an order of several grain sizes can cause significant signal changes. This information may be useful in measuring properties of the material microstructure, however, a spatial characteristic was desired for case depth measurement. To accomplish this spatial averaging was used.

Spatial Averaging

Combined effects of spatial averaging and smoothing via the moving average window is illustrated in Figure 23. Illustrated is a typical RF signal, the signal envelope of the RF signal, a moving average of the determined envelope, a spatially average envelope consisting of eight unique signal envelopes and the smoothed spatial averaged envelope using MAW. Clearly the combined effects of spatial averaging and smoothing via the MAW is advantageous. The number of unique RF signals

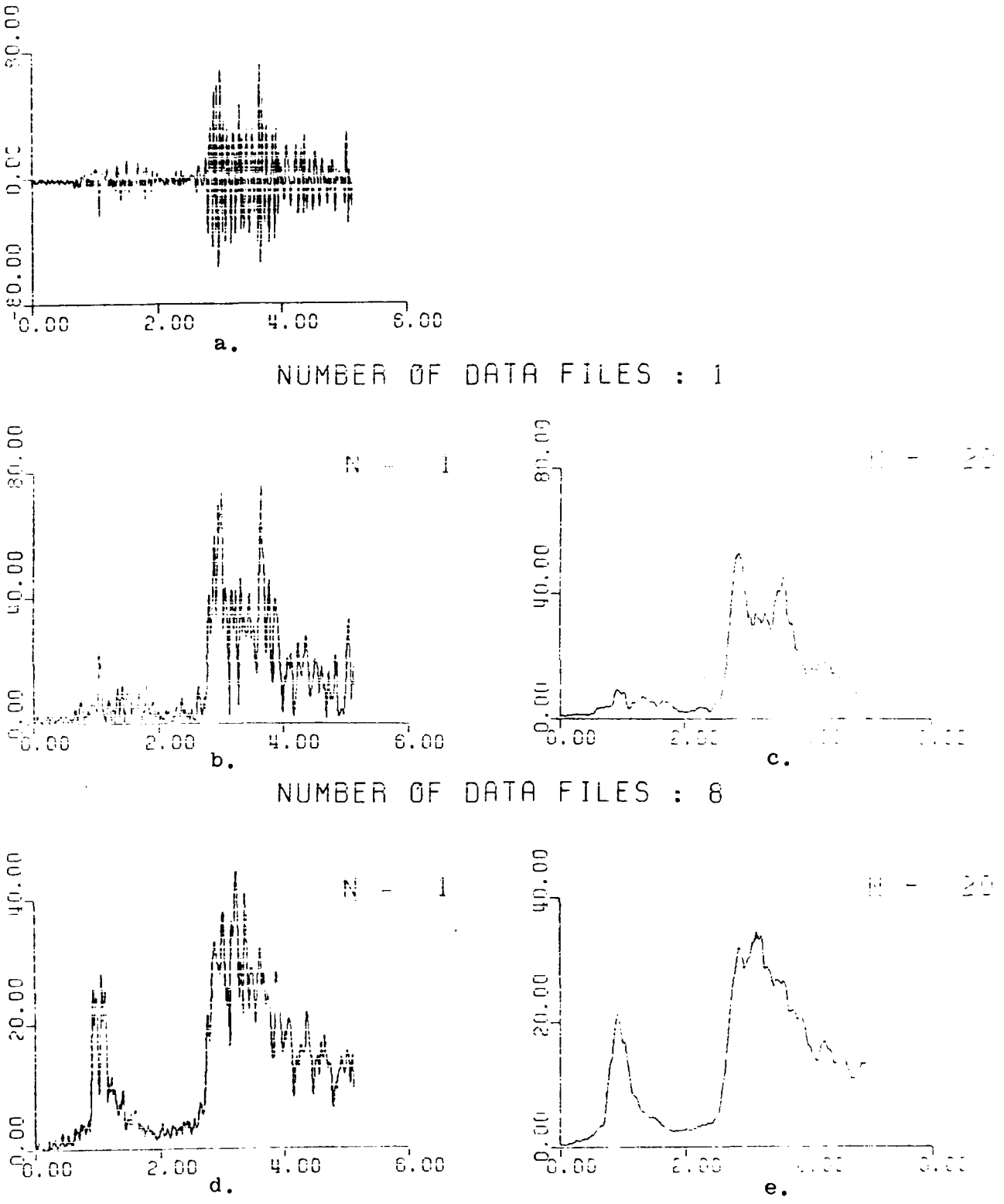

Figure 23. Affects of Spatial Averaging Combined with the Moving Average Windov

a. RF Signal, 255 Times AVeraged
b. Signal Envelope Via Hilbert Transformation
c. Smoothed Envelope Using a .19 μ Second MAW
d. Spatial Average of 8 Unique Envelopes
e. Smoothed Spatial Averaged Envelope Using a .19 μ Second MAW

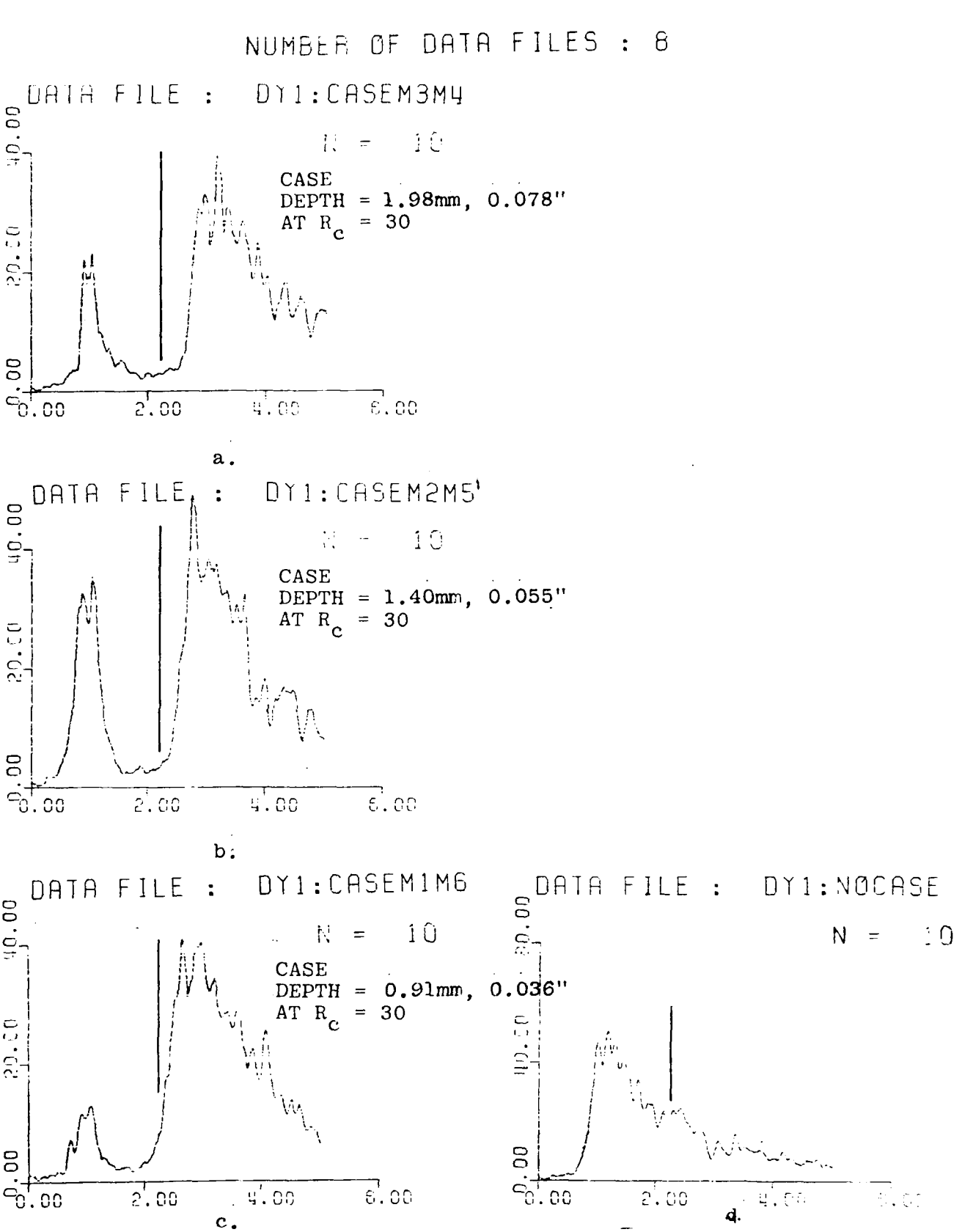

Figure 24. Comparison of Back Scattered Energy at Different Effective Case Depths. (All Envelopes determined by Spatial Average of 8 Signal Envelopes and Smoothed with .09 μ Second MAW.)

a. Effective Case Depth Equals 1.98mm or 0.030"
b. Effective Case Depth Equals 1.40mm or 0.055"
c. Effective Case Depth Equals 0.91mm or 0.036"
d. Unhardened Surface

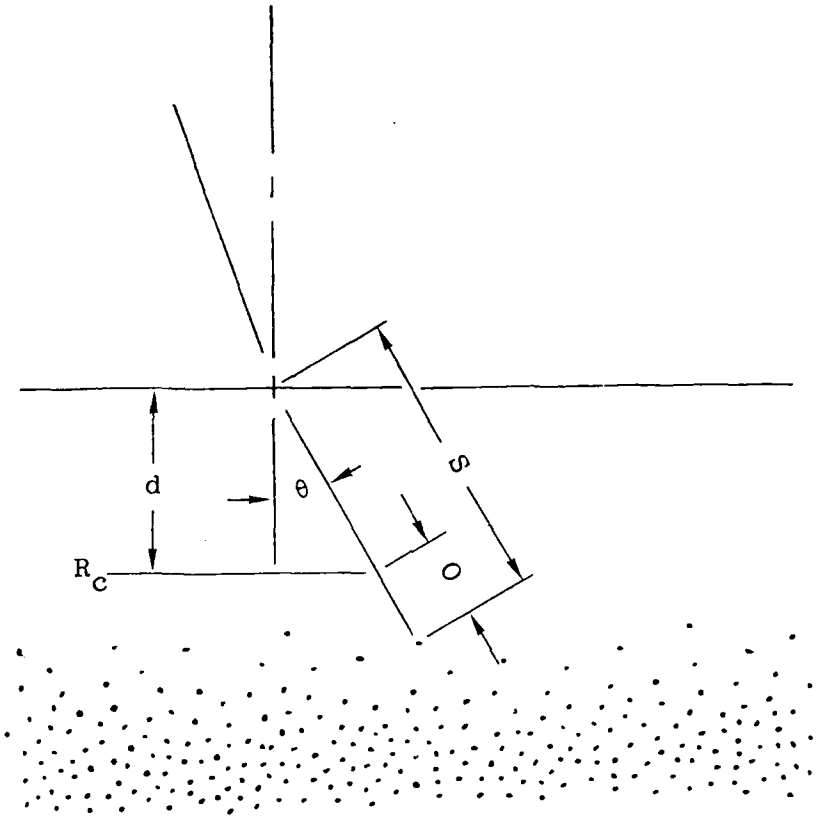

$$d = (S - O) \cos \theta$$

Let $d' \equiv$ Known Case Depth

$S' \equiv$ Known Back Scattered Distance

Then,

$$d = \frac{V_{ss}\left(T_{bs} - T'_{bs}\right)}{2} \cos \theta + d'$$

Figure 25. Model Representation of Case Hardened Specimen for Ultrasonic Pulse-Echo Angulation Determination of Effective Case Depth

to be used in the spatial average process and MAW size are determined from a consistency view point and are discussed later. At this point a procedure has been established whereby a back scattered envelope characteristic of a localized region can be determined in a manner whereby leading edge detection can be accomplished with increased sensitivity and consistency.

CASE DEPTH

Before proceeding with further analysis and ultimately with algorithm development to automatically measure case depth by the ultrasonic techniques previously described, it would behoove us to confirm our thoughts regarding expected trends. Currently the shift of the back scattered leading edge should be proportional to a relative shift in thickness of case depth. At this point no attempt has been made to associate the initiation of the back scatter phenomena with a known hardness value. The assumption made is that the two are interrelated in a proportional manner.

Expected Trends

To evaluate case depth as a function of arrival time, four graphs are presented in Figure 24. The three graphs plotted to the left represent from top to bottom, respectively, ultrasonic signatures of progressively thinner effective case depths. To aid visual preception of corresponding shifts of the back scatter energy, an arbitrary abscissa value was selected as a visual aid. Shifting of the leading edge relative to the reference point is clearly evident and confirms the basic premise that relative changes in case depth are proportional to a relative shift of back scatter arrival time. The fourth graph displays an ultrasonic signature resulting from a nonhardened surface, the opposite side of the case hardened specimen. As indicated by the graph corresponding to the unhardened surface, the leading edge occurs concurrently with the front wall echo.

Model Analysis

In our analysis of wave behavior lets assume we are the refracted shear wave entering a case hardened specimen. As we propagate through the hardened surface layer we eventually encounter diffuse scatters after traveling a distance S, Figure 25. Also, as we propagated through the steel specimen we traversed a plane characteristic of a given hardness value which segregates the effective case layer from all other material. If we measure the distance along our propagational path between the discriminating hardness plane and the point where significant back scattering is initiated and label this offset, O, the effective case depth can be determined.

Case depth can be mathematically defined by the following equation:

$$d = (S - O) \cos \theta \qquad \text{Equation (2)}$$

By using a calibration procedure where an ultrasonic signature is acquired at a known case hardened depth, d', a simple relation can be formulated as the following:

$$d = \frac{V_{ss}\left[T_{bs} - T'_{bs}\right]}{2} \cos \theta + d', \text{ where} \qquad \text{Equation (3)}$$

T_{bs} designates the arrival of the back scatter leading edge measured during the calibration procedure, and
d' is a known effective case depth corresponding to a point measured during the calibration procedure.

Note that the quantity $(T_{bs} - T'_{bs})$ relates to relative time change and therefore simplifies the case depth measuring process.

To test this model on its accuracy and consistency a series of ultrasonic measurements were performed on the case hardened specimen. However, the criteria for determining leading edge arrival time of the back scattered energy has not yet been established.

Threshold Criteria

To determine the optimal criteria for calculating leading edge arrival time seven discrete threshold values were selected at given dB levels, namely 0, 1, 3, 6, 10, 12, and 20. This action consisted of selecting the threshold value and corresponding offset value which best approximated the known case depths. Other miscellaneous points needing clarification are the number of RF signals needed for spatial averaging and the MAW gate width.

Leading Edge Determination

In determining the most consistent manner of leading edge detection, three criteria must be considered, the number of unique signal envelopes needed for spatial averaging, the MAW gate width, and the threshold. This was accomplished by use of a data base which consisted of twenty four sets of signals, eight sets for each of the known effective case depths.

Since spatial averaging is assumed to enhance the back scatter profile, Figure 24, a total of eight unique envelopes were used for each data value. This produced a data base consisting of a total of one hundred ninety-two unique signals. In optimizing the determination of the leading edge, analysis of the MAW gate size is performed followed by the threshold analysis.

MAW Gate Size Criteria

To evaluate the affects of the MAW as a function of gate size, selected values were used in conjunction with a given threshold value of 3 dB. Plots of "True Case Depth" versus "Calculated Case Depth" were used to visually inspect measurement variance and ranges of overlap between the class sets of 1.98mm, .078"; 1.40mm, .055"; and .91mm, .036". Figures 25-28, respectively, illustrate the effect of the .19, .29, and a .39 μ second MAW gate widths. Notice the reduced within-class scatter as the gate size increases. As gate size increases, however, spatial resolution is reduced. Our selection criteria becomes a gate size sufficiently large to reduce within-class scatter to an acceptable level without progressing to an overly large window.

A gate size of .29 μ seconds was selected as being optimum. This was done with the thought that the point having a true value of 0.91mm or .036" and a calculated value of 1.97mm or 0.078" was an abnormality and not characteristic of that particular data set. In this manner the .29 μ second gate was the minimal window with what was subjectively determined as an acceptable within-class scatter level.

Threshold Criteria

Plots of "True Case Depth" versus "Calculated Case Depth" were made for each of the threshold values for the MAW gate selected above and visually inspected to determine the optimum value based on the criteria of minimum within-class scatter. Figures 29-31 show graphic results for the respective threshold values of 0 dB, 6 dB, and 20 dB. Threshold value less than 20 dB were not considered since noise levels were thought to obscure signal values. The 20 dB threshold value obviously forms the best discriminating criteria for the three true case depth data sets. In using this technique only one point of the 1.39mm or .055" set overlaps the 1.98mm or .078" regime. All other points are well separated into their respective class sets.

Model Reevaluation

A reevaluation of the previous model is in order since the calculated values of effective case depth do not seem to form a strictly linear relation with true values of effective case depth. Governing reasons for this trend are thought to be associated with lateral beam resolution, beam divergence, etc.

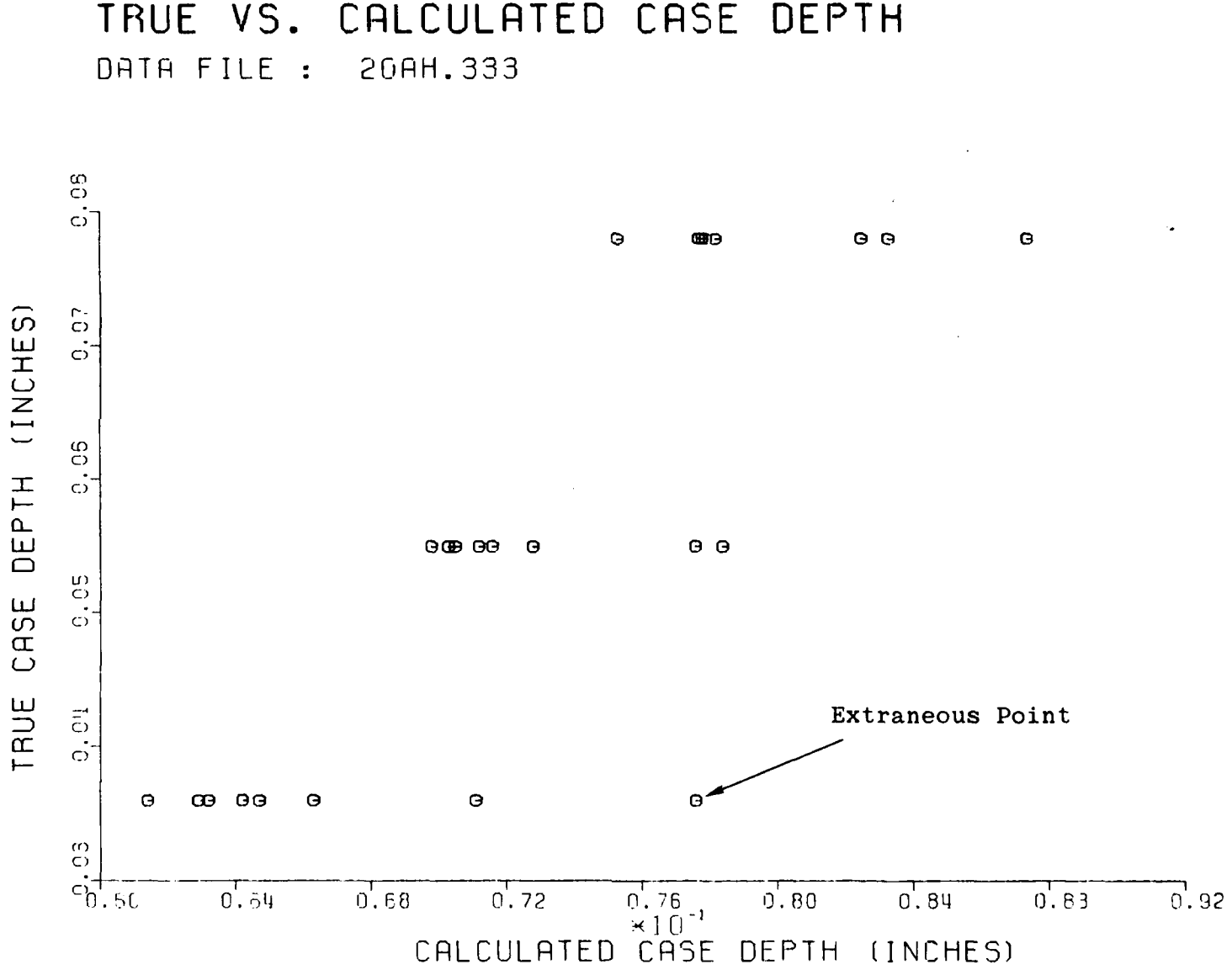

Figure 26. Graphic Display of "True Case Depth" versus "Calculated Case Depth," MAW Gate Size 0.19 μ Seconds, 3 dB Threshold.

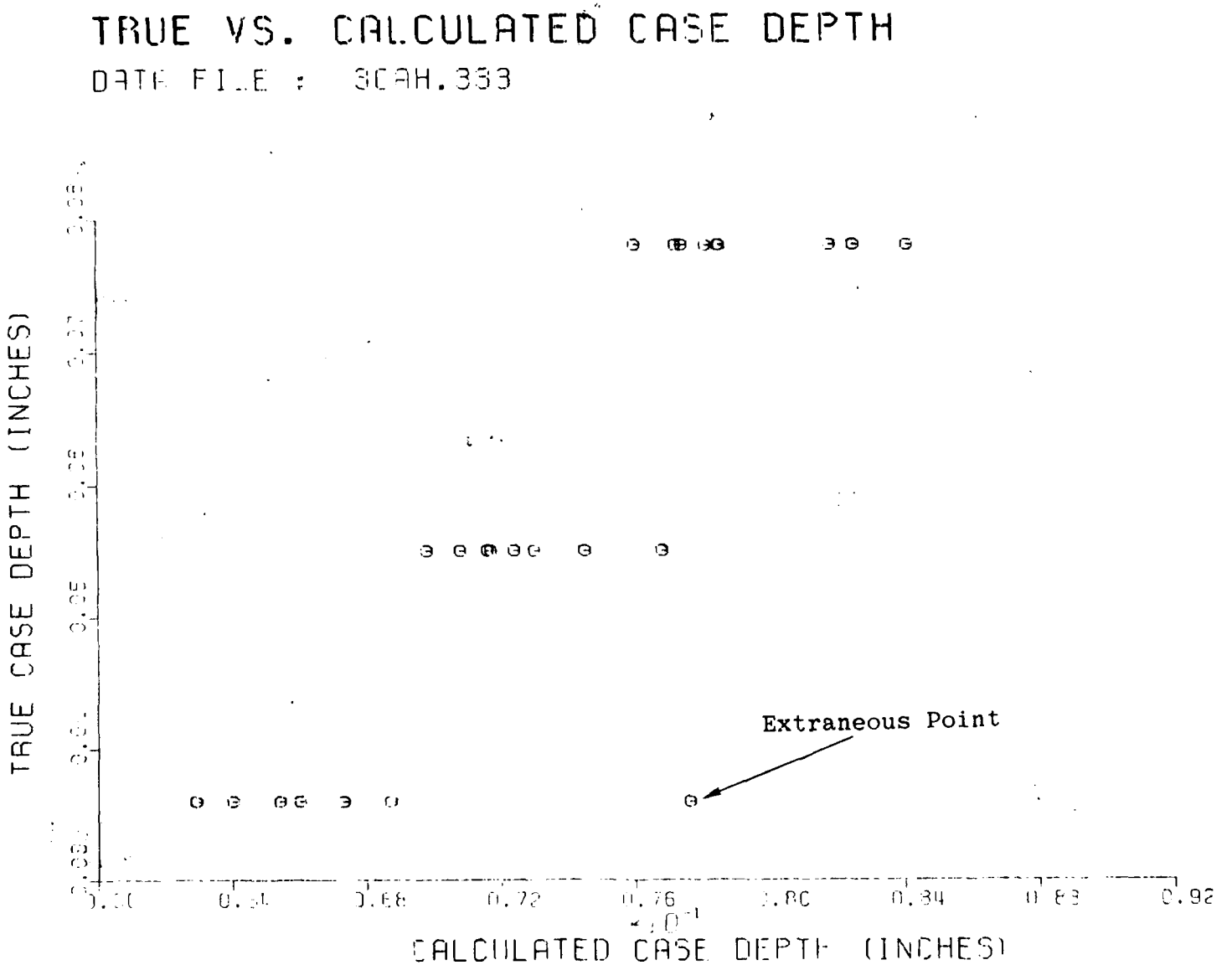

Figure 27. Graphic Display of "True Case Depth" versus "Calculated Case Depth," MAW Gate Size 0.29 μ Seconds, 3 dB Threshold

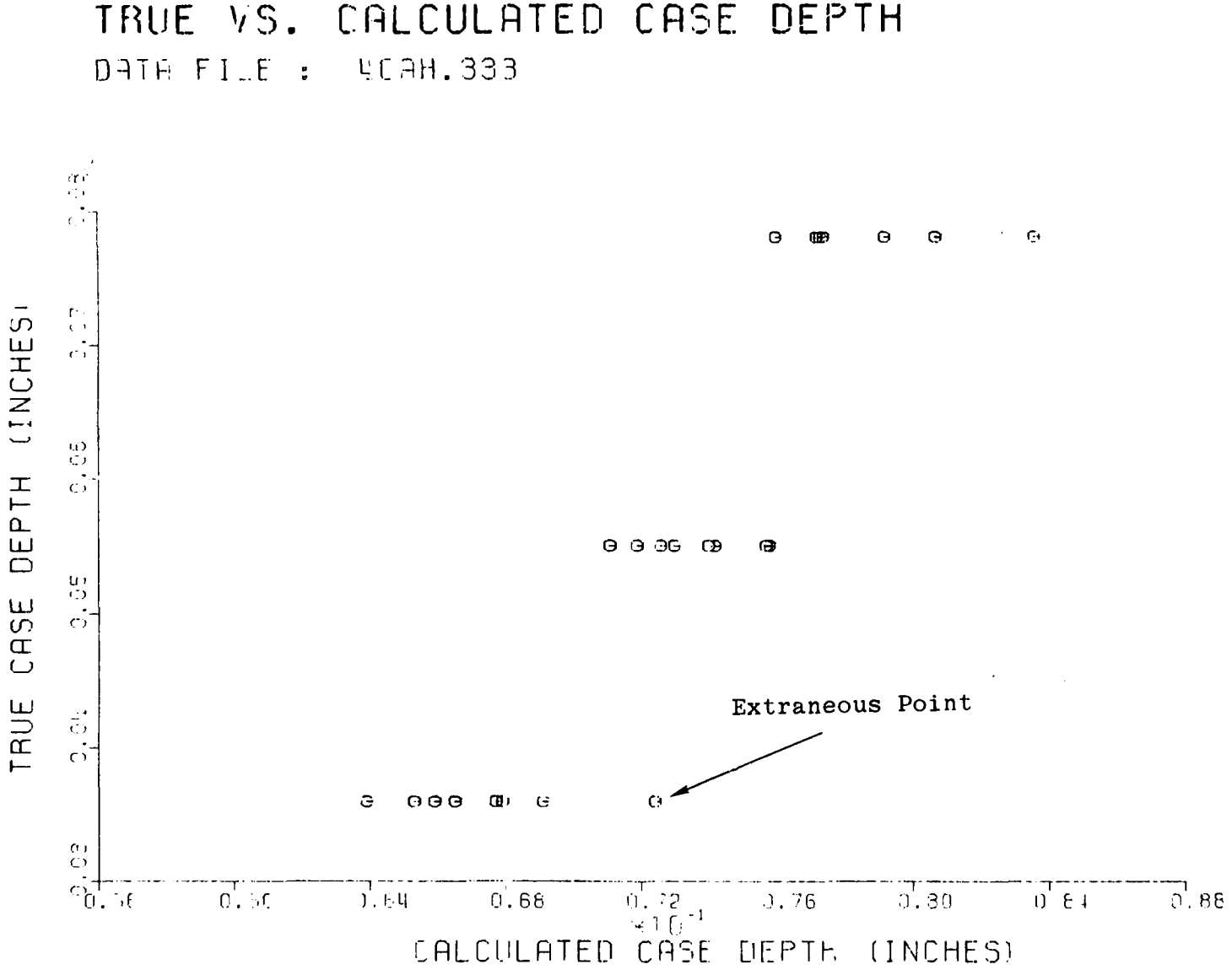

Figure 28. Graphic Display of "True Case Depth" versus "Calculated Case Depth," MAW Gate Size 0.39 μ Seconds, 3 dB Threshold

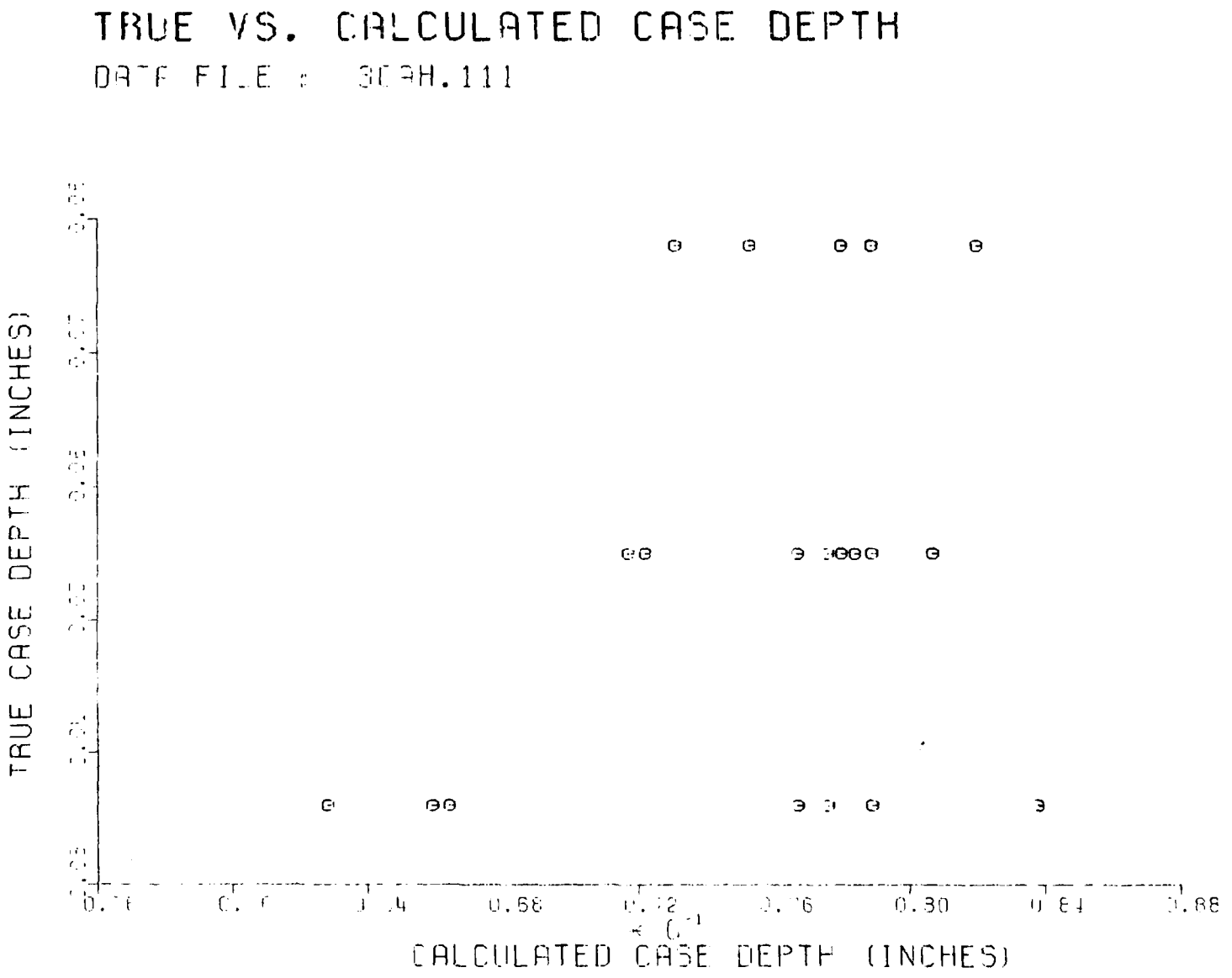

Figure 29. Graphic Display of "True Case Depth" versus "Calculated Case Depth," MAW Gate Size 0.29 μ Seconds, 0 dB Threshold

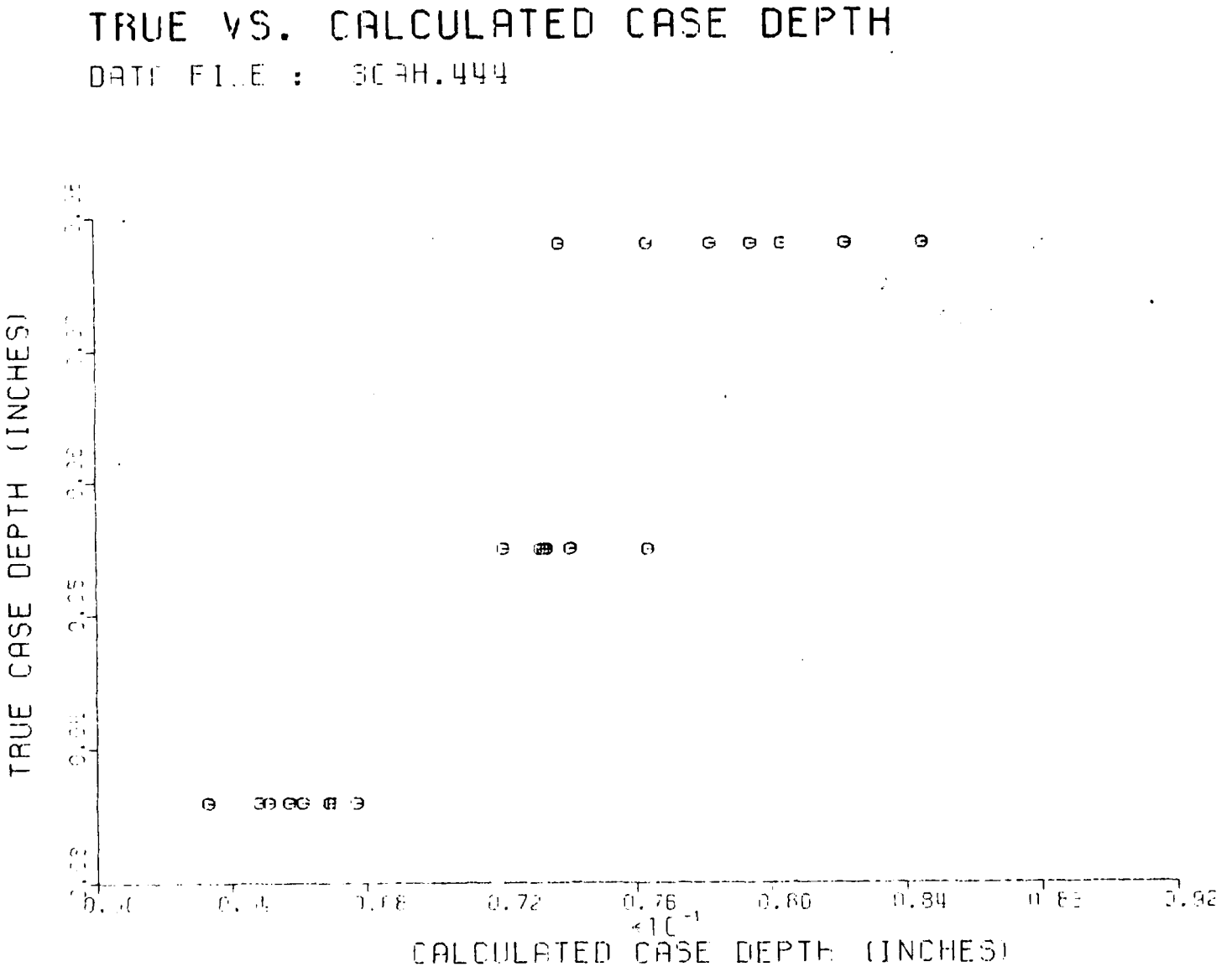

Figure 30. Graphic Display of "True Case Depth" versus "Calculated Case Depth," MAW Gate Size 0.29 μ Seconds, 6 dB Threshold

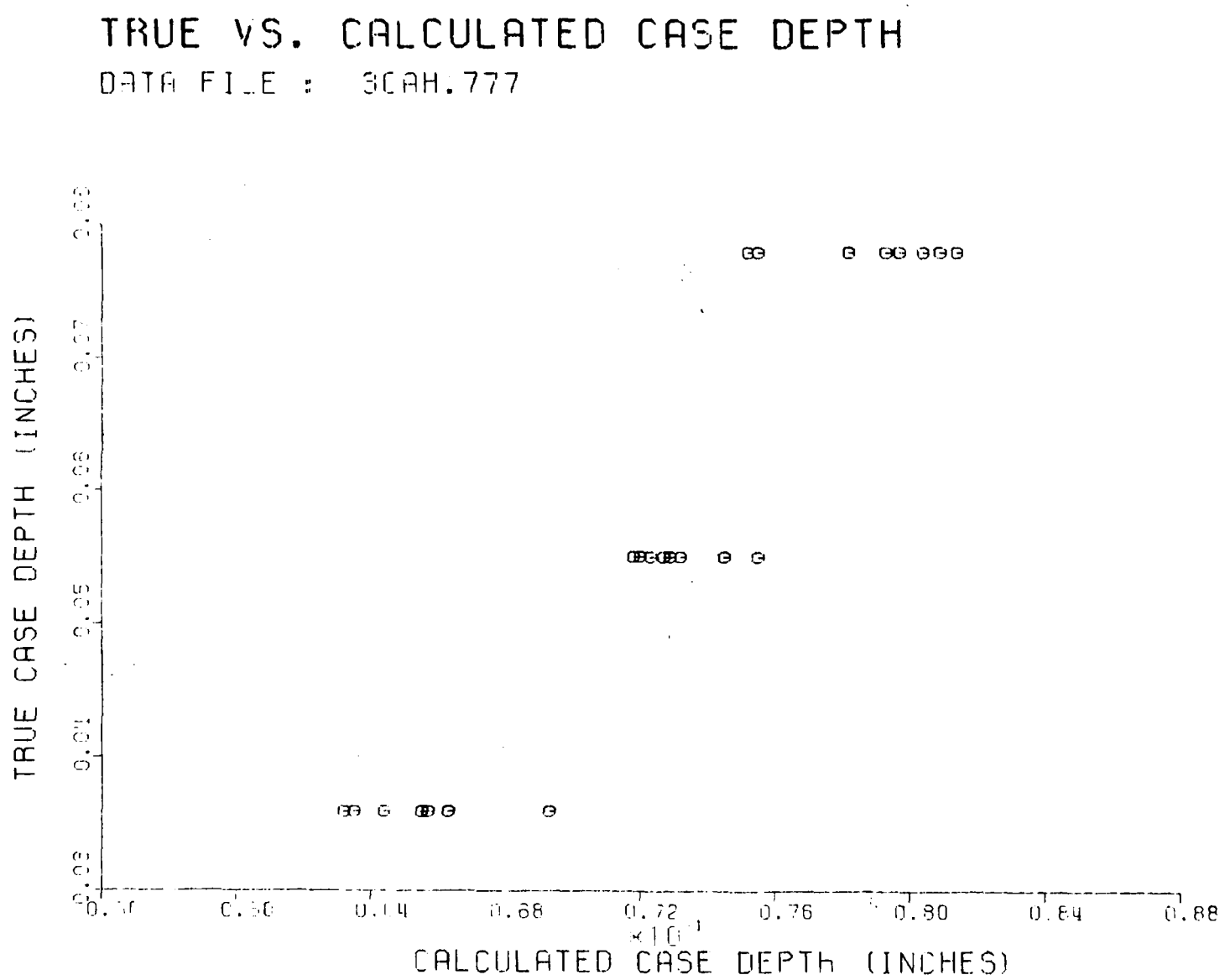

Figure 31. Graphic Display of "True Case Depth" versus "Calculated Case Depth," MAW Gate Size 0.29 μ Seconds, 20 dB Threshold

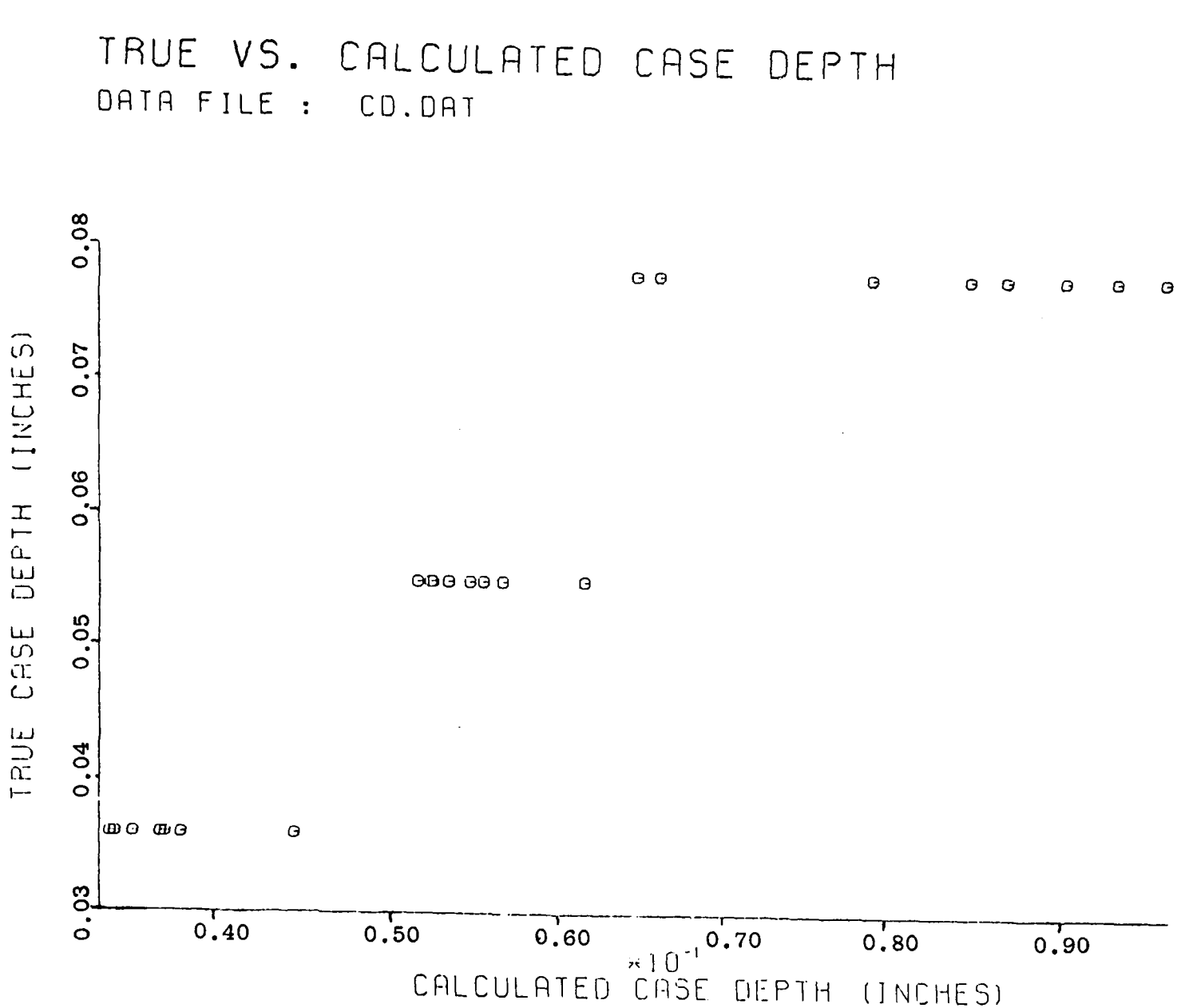

Figure 32. Graphic Display of "True Case Depth" versus "Calculated Case Depth," MAW Gate Size 0.29 μ Seconds, 20 dB Threshold, Quadratic Equation with Weights

At this time let's assume a more complicated relation exists between effective case depth and arrival time.

Since a linear relation was previously assumed, and only three known case depths are given, a quadratic equation of the form given below would be a natural choice.

$$d = W_1 (F^2) + W_2 (F) + W_3, \qquad \text{Equation (4)}$$

where,

W_1, W_2, W_3 represent respective weighting functions,

and F equals the feature value defined by the relation

$$F = T_{bs} - T_{bs}' .$$

By using the mean arrival time values determined by the .29 μ second MAW and a 20 dB threshold, the weighting coefficients can be determined. Figure 32 illustrates effective case depth determined with the weighting function. This method allows for emperical fluctuations such as lateral beam resolution, beam divergence, etc. In analyzing the data, statistical information such as the standard deviation at each of the three known case depths measurement can be used to evaluate algorithm stability, Table 4.

TABLE 4. STATISTICAL DATA ON VALUES DETERMINED FROM QUADRATIC ALGORITHM

True Effective Case Depth	Calculated Mean Value	Calculated Standard Deviation
.91mm or .036"	.94mm .037"	.25mm .010"
1.40mm or .055"	1.40mm .055"	.24mm .009"
1.98mm or .078"	2.11mm .083"	.81mm .032"

CONCLUSIONS

An algorithm has been formed which can nondestructively determine effective case depth via the ultrasonic pulse-echo angulation technique. This technique integrated various signal

processing techniques to form a relatively consistent and accurate method. Moreover, the results demonstrate that a strictly monatomically increasing relation with respect to true effective case depth exists in the regime of .91mm to 1.98mm and back scatter arrival time. This can be used as an extension of the linear relation established for large case depths of 2mm and greater. There are also reasons to believe that even thinner effective case depths such as .2mm are feasible. This is a most desirable characteristic since the methods currently used to measure case depth are restricted to limited depth ranges.

The reason for the belief that accurate measurements can be made on thinner values is due to an offset that exists between the respective planes of critical hardness and initiation of back scatter. This offset is seen as the large time difference between the front wall surface echo and the small relative time shifts corresponding to changes in effective case depth. This indicates that back scatter is initiated posterior to the discriminating hardness plane. Thus, when effective case depth equals zero a separation between the back scatter leading edge and front wall surface echo could still exist. Shift of the back scatter leading edge to the left of this point would indicate the surface hardness being less than the specified hardness value.

Prior restrictions of ultrasonically determine effective case depth were due to resolution problems caused by the extremely low signal-to-noise ratio and the apparent obscuring effect of the front surface echo. With improved signal processing techniques many of these restrictions can be relaxed. The final algorithm was able to predict effective case depth at .91mm, 1.40mm, and 1.98mm at ultrasonically calculated values of .94mm, 1.40mm, and 2.11mm with respective standard deviations of .25mm, .23mm, and .81mm. Error sources are extremely localized fluctuations in case depth, small changes in the relative position of transducer and specimen, and those relating to the ultrasonic technique used.

To date, various methods have been proposed for measuring case depth in case hardened steels. Each method as described in past literature is restricted in practical application due to problems in area localization, geometry, sensitivity, compositional variations of different steels, and compositional changes due to carbon and/or nitrogen gradients formed during the hardening process. Ultrasonic pulse-echo angulation is thought to have an inherent advantage over other methods. First, the use of focused probes allows area localization of approximately 1mm. This allows a probe to be manufactured that could easily be positioned at different localities or to be mounted on a special shoe to fit the curvature of a specimen. A restriction would apply to curvatures that would act as a distorting lens to the sound beam.

The use of eddy current is considered more severely limited with respect to area localization and as a result is susceptable to small changes in object dimensions. Eddy current is also noted to being more sensitive to near surface changes, this can be detrimental since small anterior changes can mask the measurement of case depths posterior to the surface variation. Ultrasound is not affected by dimensional changes and is relatively less sensitive to the compositional changes of different steels and localized gradient changes resulting from nitrogen and carbon which are commonly used in the hardening process.

Feasibility for development of an ultrasonic device for measuring effective case depth in case hardened steels has been shown. This is due to the added range of case depths that ultrasonics can measure, area localization, relatively insignificant signal distortion due to depth, relative stability regarding material composition, and especially the potential for further technique refinement. More work is needed to reduce the scatter of measurements of thin case depths and to more firmly establish the previously defined relations. This work can be defined in two parallel efforts, first increased signal processing via software to establish optimum methods and second, the acquisition, integration, and possibly the development of state-of-the-art electronic instrumentation. This would enhance the signal-to-noise ratio causing better analysis and possibly lead to a purely analog instrument that would greatly expedite testing procedures. The two processes, of course, would have feedback such that the best in both microprocessors and analog circuitry would be combined. Extensive studies regarding different steels, hardening procedures, and degrees of hardness are recommended for future technique refinement in consistency, particularly thin case depths, calibration, and defining limiting conditions.

REFERENCES

1. Emerson, P. J., "Alternative Methods for Measuring Case Depth in Ferrous Components," British Journal of NDT, Vol. 18, No. 2, March 1976.

2. Perenne[illegible], C., Chretien, N., Gaillot, D., "Nondestructive Te[illegible]ing of Hardening Depth in Steel Cylinders by Two Ultrasonic Methods," Proceedings of Ninth World Conference on Non-Destructive Testing, Se[illegible]sion 1B-2, November 1979.

3. Beech, H. G., "The Problem Solved - or Has It?," British Journal of NDT, Vol. 18, No. 2, March 1976.

4. Taylor, J. L., "An Intoduction to Case Hardening Processes," British Journal of NDT, Vol. 18, No. 2, March 1976.

5. Flambard, C. and Lambert, A. "Measuring the Chill Depth by Ultrasonic Waves," CETIM Information, April 9-17, 1973.

6. Goelbels, K. "Structure Analysis by Scattered Ultrasonic Radiation," Research Techniques in Nondestructive Testing Vol. IV, Chapter 4, Academic Press, New York, 1980.

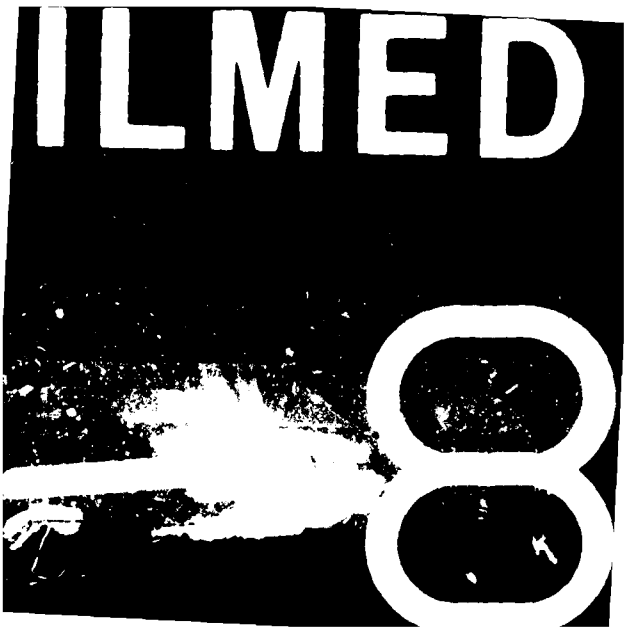
ILMED
8